UNIVERSITA' DEGLI STUDI DI PADOVA

FACOLTA' DI INGEGNERIA
DIPARTIMENTO DI MECCANICA

TESI DI LAUREA MAGISTRALE (LM) IN
INGEGNERIA DEI MATERIALI

AMBIGUOUS SURFACES FOR BIOFOULING RESISTANT, HIGH FOULING RELEASE POLYMER COATINGS

Relatore: Prof. Massimo Guglielmi
Correlatori: Prof. Edward J. Kramer, Dott. Michael D. Dimitriou

Laureando: NICOLA BRAGAGNOLO

ANNO ACCADEMICO 2010 – 2011

To my Mother and Father for their undying support

Contents

1 Antifouling Casting..... 1

1.1 Issues about fouling on the hull..... 1
1.2 historic antifouling methods..... 5
1.3 Modern Antifouling alternatives..... 6
1.4 Booster Biocides Approach..... 8
1.5 Foul Release Approach..... 8
1.6 Antifouling systems — universal approaches..... 10
1.7 Macromelecule surfaces..... 12
1.8 Functional polymers..... 14

2 Experimental section.....17

2.1 DLS..... 18
2.2 AFM..... 21
2.3 Water Contact Angle..... 25
2.4 XPS..... 26
2.5 Prep of the solutions, GPC and DLS..... 32
2.6 Spin coating technique..... 34
2.7 Annealing in the oven..... 37

3 Results and Discussion..... 38

3.1 DLS (graphs, discussion)..... 38
3.2 AFM..... 48
3.3 Second System PS-b-P(EO-AGE)..... 53
3.4 AFM (images, discussion)..... 54
3.5 Water contact Angle (data, graphs, discussion)..... 56
3.6 AFM (AGE and fAGE)..... 60
3.7 XPS (graphs, discussion)..... 64

4 Conclusion..... 74

Bibliography..... 77

Chapter 1

Antifouling Coatings

Issues about fouling on the hull

Engineered structures such as ships and marine platforms, as well as offshore rigs and jetties, are under constant attack from the marine environment. These structures need to be protected from the influences of the key elements of the marine environment such as saltwater, biological attack and temperature fluctuations.

Besides injectable biocides in closed systems, methods of protecting marine structures must be capable of expanding and contracting with the underlying surface, resist the ingress of water and control the diffusion of ions. Protective organic coatings can offer these functions and consequently are largely used in the shipping industry to increase the working life of systems and improve its reliability.

Paint coatings on ships are used for a wide range of functions such as corrosion resistance, ease of maintenance, appearance, non-slip surfaces on decking as well as the prevention of fouling on the hull by unwanted marine organisms.

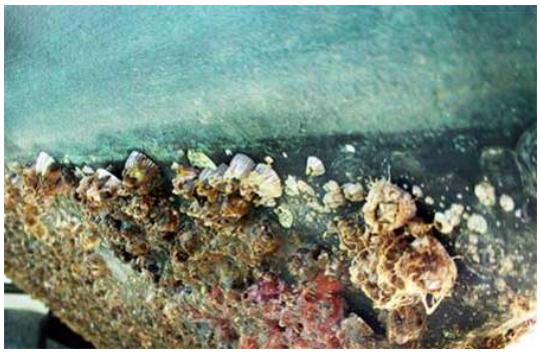

Figure 1.1: Fouling example on a hull.

The use of antifouling coatings for protection from the marine environment has a long history. By considering the historical and current approaches to antifouling systems, I will introduce the use of modern approaches to the design of an environmentally acceptable, broad spectrum antifouling system for a large ship's hull.

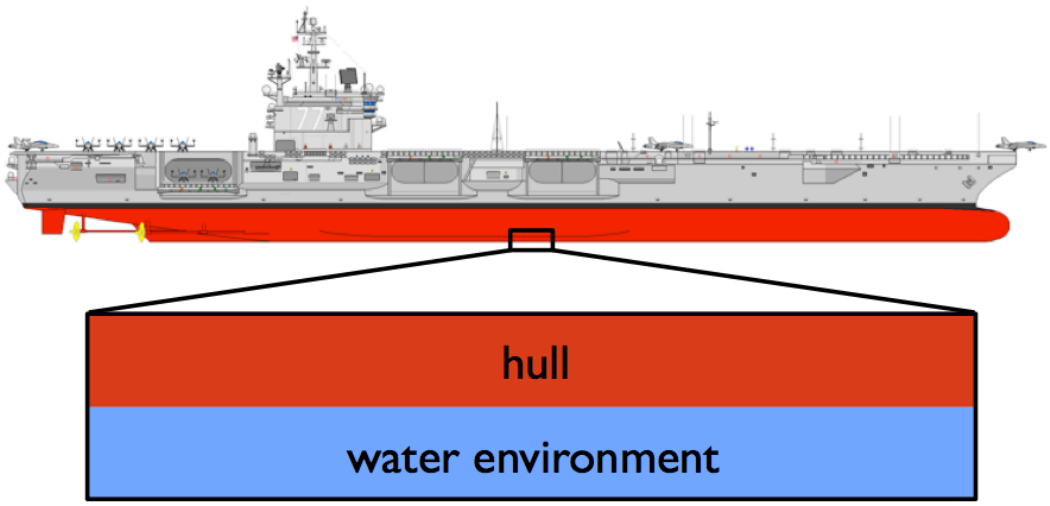

Figure 1.2: large ship hull.

The settlement and accumulation of marine organisms on an inanimate substrate can cause large penalties to engineered structures. In heat exchangers, biofouling can clog systems and on ship hulls it can increase the hydrodynamic drag, lower the manoeuvrability of the vessel and increase the fuel consumption. This leads to increased costs within the shipping industry through the increased use of manpower, fuel, material and dry docking time.

The process of biological fouling is often grouped in the literature into key growth stages which include an initial accumulation of adsorbed organics, the settlement and growth of pioneering bacteria creating a biofilm matrix and the subsequent succession of micro and macrofoulers (Fig. 1.3).

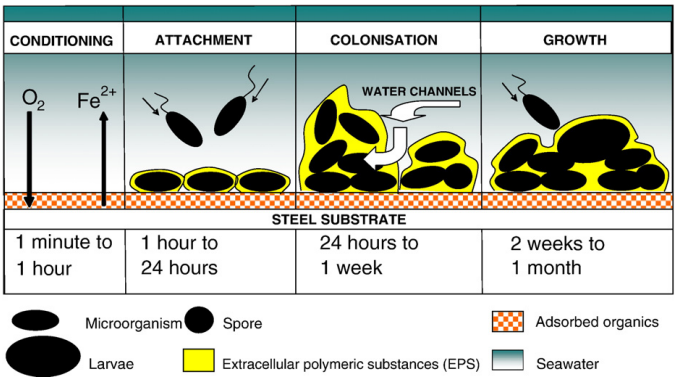

Figure 1.3: Schematic of critical biofouling stages.

The sequence of biofouling is not predictable due to the exploitation of substrate niches by higher fouling organisms. Biofilm formation is often a precursor to subsequent fouling by macrofoulers. The succession of biofouling has been experimentally tested by removing initial algal layers resulting in limited further fouling. The presence of a biofilm has been recorded to have a positive influence on the settlement of some algal zoospores, whereas Faimali et al. recorded that an aging biofilm inhibited the settlement of barnacles.

When a chemically inert substrate is immersed in seawater an almost immediate accumulation of organic carbon residues adsorb onto the wetted surface, composition of which depends on the ions, glycoproteins, humic and fulvic acids available in the liquid phase. The forces that promote the adsorption and conditioning of the surface include electrostatic interactions and Van der Waal's forces.

Pioneering microorganisms can now attach to the surface forming a biofilm. Contact and colonization between the microorganism and the surface is promoted by the movement of water through Brownian motion, sedimentation and convective transport.

Bacteria and other colonizing microorganisms secrete extracellular polymeric substances (EPS) to envelope and anchor them to the substrate thereby altering the local surface chemistry which can stimulate further growth such as the recruitment and settlement of macroorganisms.

The adhesion techniques employed by fouling organisms are diverse and can often be a two-component process with both temporary and permanent adhesion.
In a similar manner, the common macroalgae Ulva sp., has a temporary and permanent attachment phase to its lifecycle.
The adhesion of species to a substrate is an important aspect of biofouling for if this process could be prevented, fouling could be controlled. Adhesion and settlement is also often a key stage in the life cycle of marine organisms, so the evolutionary pressure to colonize a surface is great. The driving force of adhesion can be considered as being made up of contributions from the interfacial tension between the organism and the substratum, organism and the liquid and between the substratum and the liquid.
Biofouling exploits ecological niches on a ship's hull, generating varying settlement densities. This can lead to manoeuvrability penalties in specific (e.g., propeller fouling) and non- specific ways (e.g., water line fouling). A vessel's sound signature is also affected, by this degradation of a ship's performance, forboth passive and active sonar systems.

A variety of materials can be used for ship hulls including steel, aluminum and composites such as glass-reinforced polymer. The fouling of ship hulls is often prolific as vessels move between a diverse range of environments and remain constantly in the most productive region, the photic zone, of the water column. Although coatings are used for hull protection, they can fail due to the build up of inorganic salts, exopolymeric secretions, and the calcium carbonate skeletal structures that form the fouling organisms.
There are penalties associated with the unwanted colonisation of a hull surface by marine organisms, for example, hydrodynamics are negatively affected. A hull is subject to both form drag and skin friction drag as the vessel navigates through water. Biofouling affects the latter by increasing the average hull roughness and wall shear stress. The effects of antifouling coatings, such as self-polishing copolymer (SPC) and foul release coatings (FRCs), on the hydrodynamic boundary layer have been shown to have little influence on either its thickness or shape factor, although friction velocity was increased.

Biofouling exploits ecological niches on a ship's hull, generating varying settlement densities. This can lead to maneuverability penalties in specific (e.g., propeller fouling) and non- specific ways (e.g., water line fouling). A vessel's sound signature is also affected, by this degradation of a ship's performance, for both passive and active sonar systems.

Historic antifouling methods

The use of toxic antifoulants on ship hulls has been a historic method of controlling fouling but biocides such as lead, arsenic, mercury and their organic derivatives have been banned due to the environmental risks that they posed.

A revolutionary self-polishing copolymer technique employing a similar heavy metal toxic action to deter marine organisms was used with the antifoulant tributyltin (TBT). Antifouling systems that do not use heavy metals are the foul release coatings.

The use of organotins was eventually banned. In the 1980s it became apparent that the use of TBT was causing severe damage to non-target species in the wider marine environment, such as deformities in shellfish and mollusca communities, reduced growth of algae and toxic effects in young fish.

The majority of anti-fouling coatings also contain solvents which are harmful by inhalation and by skin or eye contact. They can have a narcotic effect resulting in the following symptoms: headache, dizziness, irritability and mental confusion. These reasons brought out the question of using TBT based AF paints further.

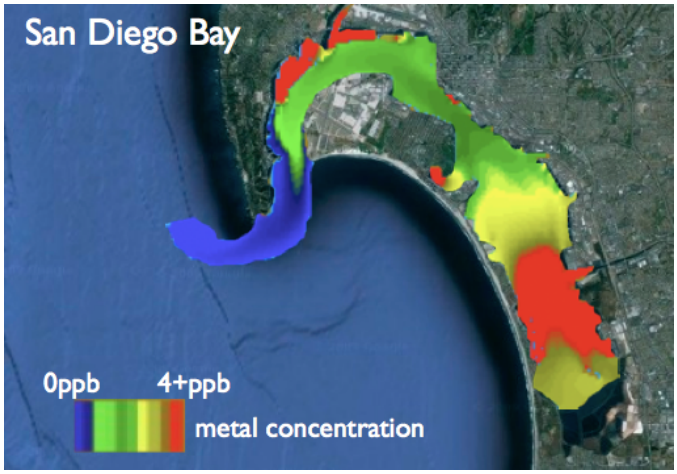

Figure 1.4: San Diego Bay metal concentration.

However, in November 1998 the IMO made the decision to introduce a world-wide ban in the use of TBT in antifouling paints for most ships from January 2003. In 1999 the International Maritime Organization (IMO), the United Nations Agency concerned with the prevention of marine pollution, agreed a resolution which calls for:

1) A global prohibition on the application of organo-tin compounds acting as biocides, in anti-fouling coatings on ships by 1 January 2003;

2) A complete prohibition on the presence of such compounds, in anti-fouling coatings on ships by 1 January 2008.

The ban of TBT based AF paints by IMO made the ship industry to think of cost effective non polluting paints to fight against bio-fouling and bio-corrosion.

Thermoplastic, non-convertible surface organic coatings, which dry due to simple solvent evaporation, are today readily available although volatile organic compound (VOC) controls are limited in antifouling applications.

The development of antifouling systems has a long history but the last ten years has seen an increase in the focus on environmentally acceptable alternatives.

Modern antifouling alternatives

Many traditional antifouling systems are “paints”, which is a comprehensive term covering a variety of materials: enamels, lacquers, varnishes, undercoats, surfacers, primers, sealers, fillers, stoppers and many others. Antifoulants are one of many additives usually incorporated within the topcoat paint of a marine protective coating system. The average theoretical spreading rates for commercially available antifouling systems for naval applications is considered to be around 6.2 $m^2 L^{-1}$ at 93 μm dry film thickness, with the majority utilizing two coat applications. Most antifouling coatings are organic and consist of a primer and a topcoat both of which can include anticorrosive functions, however, the topcoat is often porous.

The ban on TBT in 2003 created a gap in the market and research began into environmentally acceptable replacements as reviewed elsewhere. In the interim, other metallic species, such as copper and zinc are in current use as substitutes and are delivered in a modified self-polishing copolymer delivery mechanism. The selfpolishing copolymer (SPC) technique uses both hydrolysis and erosion to control the antifouling activity. Seawater ingress allows for the hydrolysation of the antifouling compound from the polymer backbone and the coatings solubility leaves the surface polished. This controlled dissolution of the surface of the coating allows for a longer lifetime.

There are two alternative key techniques for controlling the release of antifouling compounds from a coating by using either a soluble or insoluble matrix (Fig. 1.5).

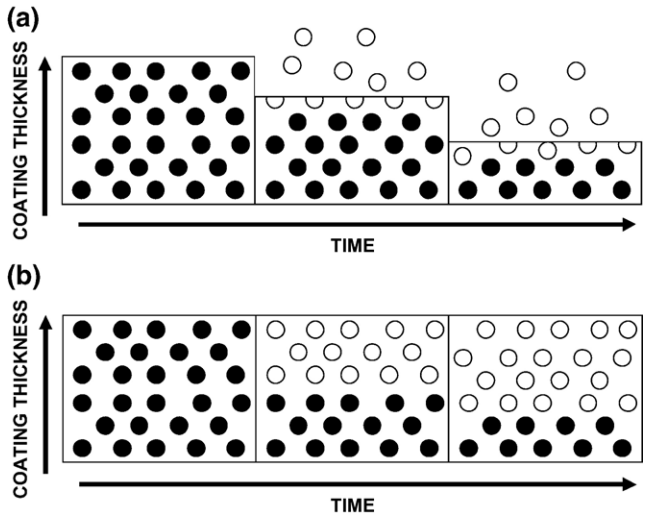

Figure 1.5: Schematic of (a) soluble matrix biocide releasing coating and (b) insoluble biocide releasing coating. ● Antifoulant loaded, ○ depleted antifoulant.

Controlled dissolution of antifouling compounds is difficult and copper toxicity is under recent scrutiny. Copper is found naturally in the marine environment at high concentrations and is relatively benign to humans although Environmental Protection Agency (EPA) regulations for drinking water stipulate a limit of 1000 $\mu g\ L^{-1}$. Comparatively, concentrations as low as 5–25 $\mu g\ L^{-1}$ can be lethal for marine invertebrates. The biomagnification of sequestered copper species through the trophic levels, however, could potentially have an effect on the food

industry. Heavy metals are often toxic to marine organisms and humans due to the partitioning of metabolic functions. The reticent use of heavy metals to control fouling in the marine environment due to the TBT ban and increased legislation on toxicity requirements is being replaced in favor of alternative approaches.

Booster biocides approach

As well as increased skepticism over the use of copper, an increased tolerance has been reported for a select group of macrophytes including the key fouling algal species Enteromorpha (now Ulva). As a result, booster biocides have been incorporated to increase the length and functionality of copper-based antifouling coating systems. Two of the key booster biocides (Irgarol 1051 and Diuron) have been regulated by the UK Health and Safety Executive with Diuron banned from application and Irgarol restricted to application on vessels greater than 25 m in length. Terrestrial pesticides have also been adapted for marine antifouling systems but have increasingly had issues with their persistence and toxicity. This approach is often too species specific or conversely too broad, influencing non-target organisms. The effectiveness of the copper-based coatings is restricted by the ability of the coatings to consistently leach the booster biocides. The concentrations of biocide released in free association paints (whether soluble or insoluble) requires better control; also their persistence in marine sediments due to such mechanisms as incorporation within degraded paint particles needs continued monitoring.

Foul release approach

Foul release coatings (FRCs) function due to a low surface energy, which degrades an organism's ability to generate a strong interfacial bond with the surface. The smoothness of the coating at the molecular level allows for organisms to be dis-lodged once the vessel is moving beyond a critical velocity, i.e. typically 10–20 knots ship speed, depending upon the fouling community. These non-stick surfaces aid removal of fouling through shear and tensile stresses as well as their own weight by lowering the thermodynamic work of adhesion.

A combination of the critical surface free energy (22–24 mN m^{-1}) and low elastic modulus allows the interface/joint between the organisms adhesive and the coating surface to fracture and fail. The adhesion of a marine fouling organism to a wetted substrate creates two surfaces, the surface adhesive interface and the adhesive water interface. As described earlier it is these interfacial tensions, which control the organisms' ability to adhere.

There are two key types of FRCs, namely fluoropolymer and silicone based polymer coatings. The application thickness of silicone coatings is typically 150 μm in comparison with 75 μm for fluoropolymers. The thickness of the coating allows for the coating modulus to be controlled. A thicker coating as seen with the silicone elastomers is more successful as it requires less energy to fracture the bond between the foulant/coating. Removal of the attached organism occurs through a peeling fracture mechanism as opposed to the shearing associated with the harder, thinner coatings of the fluoropolymer coatings.

Low form biofoulers like diatoms are especially tenacious and are difficult to remove from foul release coatings. The implication of this is that the removal of diatomaceous slime from the non-stick coatings when the vessel is in transit is difficult.

The purely physical deterrent effects of these low energy coatings provide a unique approach to developing an environmentally acceptable alternative to biocide-based antifoulants. It offers a broad spectrum antifoulant without incurring the issues of biodegradation, legislative standards and fees necessary to register an active antifouling compound. This is an effective passive means of approaching the aggressive marine environment. However, the tenacity of biofilms increases the critical speed velocity needed to dislodge the foulers. As this approach does not tackle biofouling while the vessel is berthed dockside, biological communities are allowed to establish and macrofoulers can then be translocated biogeographically causing environmental issues of alien species transport. The negative effects of alien species on native biological communities include the competition for ecological niches eradicating indigenous species and generating issues for local biodiversity and aquaculture. There are also issues with the toxicity of the silicone oils in the dockyard and the use by some silicone based

paints of the curing agent dibutyltin laureate. This organotin catalyst may contain TBT and monobutyltin (MBT) compounds. FRCs are not a universal antifouling solution for ship hulls and require certain operational profiles to function efficiently. The penalty of increased fuel consumption until the vessel does 'release' the biological foulers has yet to be investigated thoroughly.

Further antifouling coatings

A wealth of alternatives have been initially investigated for various marine applications to replace the use of TBT.

The process of surface flocking is where electrostatically charged fibers are adhered to a coating perpendicular to the surface and is currently undergoing trials as an antifoulant mechanism.

The fibers can be made of polyester, polyamide, nylon or polyacryl. Using nylon fibres on a polyvinylchloride plastic sheet a decrease in green algae and barnacles was recorded for a 6 month field trial.

Other non-toxic coatings have been developed such as the two coat systems of basecoat polybutadiene or urethane and a topcoat of silicone or hydrocarbon. All five two coat systems were fouled by slime and algae but were resistant to fouling by barnacles and bryozoans in field trials 6–12 months in length. Alternative surfaces that resist bioadhesion such as short chain PEG have been investigated as well as alternative surface architecture to resist protein adsorption.

Antifouling systems — universal approaches

There are three key aspects (Fig. 1.6) that need attention, the engineered protective coating bounded on either side by the substrate and the environment, both of which have unique properties that will affect coating integrity and effectiveness.

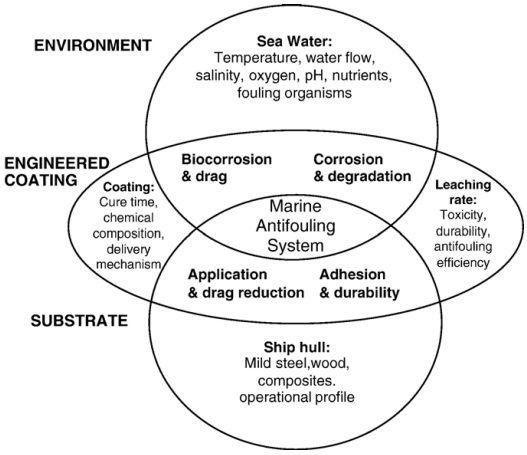

Figure 1.6: Key interactive parameters affecting an antifouling coating system.

The requirements needed for an optimal antifouling coating are:

Anticorrosive Antifouling;
Environmentally acceptable;
Economically viable Long life;
Compatible with underlying system;
Resistant to abrasion/biodegradation/erosion;
Capable of protecting regardless of operational profile;
Smooth;

and it must not be:
Toxic to the environment;
Persistent in the environment;
Expensive;
Chemically unstable;
A target for non-specific species.

Additional factors that need to be considered include its life cycle parameters and measurable effectiveness, which incorporate toughness, erosion and release of the antifouling compound.

Protection of hull of a ship is one of the most challenging factors. Even a minute corrosive element can cause a tremendous loss to the ship. As mentioned, the paints used to prevent the bio-fouling are toxic to marine environment. If the anti-fouling paints are not used then it will lead to bio-corrosion, as well as increased hull resistance and in turn increased fuel consumption. So antifouling coatings are important as long as life of ship and sea trade is concerned. Anti-fouling hull coating system can provide substantial environmental benefits and a way to save money. But the methods employed may cause severe damage to the environment.

At present there are regional, national, and international regimes in place to control the detrimental effects of anti-fouling coating systems. This is because there is a compelling need to minimize the environmental harm caused by the biocides employed.

Although there is some less toxic alternative biocide under consideration, some of the most promising alternatives may be those that approach the problem by inhibiting adherence of the species to the hull rather than killing the species directly.

Macromolecular surfaces

Due to the vast array of chemical moieties and architectural structures accessible through polymer chemistry, synthetic polymers enable one to engineer a vast range of polymer properties. This breadth of physical properties combined with inexpensive processing conditions make polymers highly competitive with other materials for a diverse set of applications. The variety of methods by which polymers can be efficiently and effectively deposited onto a surface has established them as ideal materials for the coatings industry.

The chemical and structural composition at the surface of a polymer dictates many of its measurable properties. Hence, tuning the surface of a polymer can lead to controlled interactions between the polymer surface and the external environment. Capitalizing on certain interactions can prompt the development of

specialized coatings that satisfy industrial needs in a variety of applications. Some examples include coatings for antireflection, non-stick, antifouling, antimicrobial, self healing, abrasion resistance, and chemical resistance. Each coating utilizes different material properties that define the overall surface character and consequently the performance of the coating as a whole.

With increasingly stringent regulations on antifouling coatings, a need has been identified for new, robust, environmentally-friendly materials to be developed that inhibit attachment and prevent biofouling. Diverse polymer functionality employable through modern synthetic methods and ease of polymer deposition over large areas identifies them as promising materials for this challenge.

The structure at the surface of a polymer is not necessarily the same as its structure in the bulk. Preferential interactions between the surface and a chemical moiety in a polymer system will affect its structure at the surface. For example, when two polymers are blended, the system can reduce its total free energy by increasing the composition of the the lower surface energy polymer at the blend/air interface.

There have been numerous reports investigating surface enrichment of polymer blends and multicomponent systems such as block copolymers. From a processing standpoint surface enrichment is important because the bulk properties are not always representative of the surface properties of a polymer and this gives engineers a handle to tune surface and bulk properties separately. By throughly understanding this phenomenon it is possible to attain increased control over the final properties in a polymer system, however, additional physical properties such as surface energy, interaction parameters, molecular weight, architecture, and processing conditions must be considered.

To harness this control an array of polymer architectures have been developed with the ever growing toolbox of synthetic techniques and strategies in the chemistry community. Figure 1.7 highlights some general architectures that have been used to mediate interfacial interactions not only at the surface of a polymer, but also at the substrate, and between two distinct polymer phases. With the advent of block copolymer architectures and the industrial demand for smaller

feature sizes and higher aspect ratios, interfacial considerations are now more important than ever.

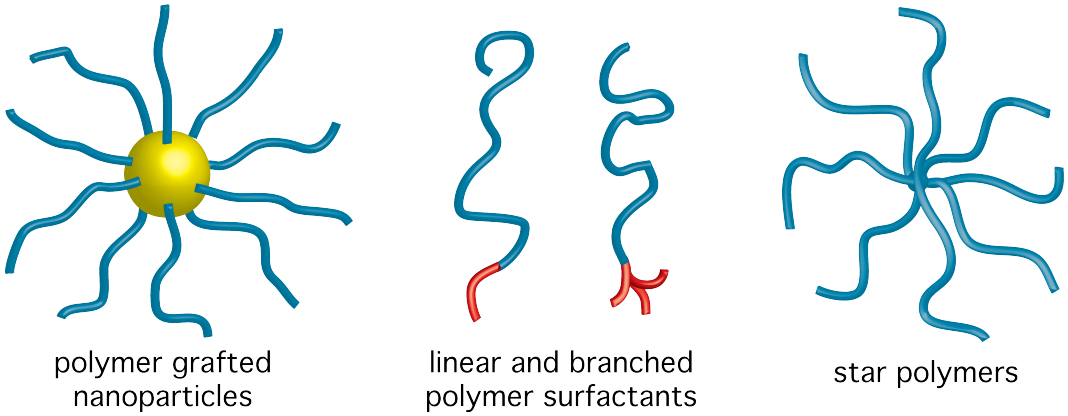

Figure 1.7: Three examples of additives that segregate to interfaces to mediate interfacial interactions.

In block copolymers the architectures illustrated in figure 1.7 have been used to induce a number of effects including substrate/surface wetting, microphase separation, directional ordering, and emulsion formation.

Functional polymers

When there is a desire to alter surface interactions, perfluorocarbons are a promising candidate and have been identified as a unique set of organic molecules that vastly broaden the industrial applicability of polymers. They offer a range of useful properties such as high transparency, thermal resistance, and chemical resistance, and are low in surface energy, refractive index, and dielectric constant. However, perfluorocarbons do not readily undergo chemical modifications. The high electronegativity of fluorine atoms changes the reactivity of nearby functional groups, and their oliophobic and hydrophobic nature means they have low solubility in common non-hazardous organic solvents. Solubility issues are exacerbated in perfluorocarbon containing polymers, making them especially hard to process.

With the advent of controlled free radical polymerization methods, it has become easier to incorporate precise and manageable amounts of perfluoro-carbons into

polymer systems. Thus, polymer processing has become ultimately easier as systems can be designed with smaller amounts of perfluro-carbons where needed. Additionally, different polymer architectures can be synthesized that incorporate perfluorocarbons. Figure 1.8 depicts two of the more common architectures used in this work. The top structure is accessible through the copolymerization of a given monomer with a perfluoro-functional monomer to give a statistical copolymer. This copolymer could then be part of any larger scale macrostructure such as block copolymer as it is depicted in figure 1.8.

A second strategy is to end functionalize a polymer chain with a perfluoro-functional moiety, forming a polymer surfactant (bottom). This surfactant could act alone or be blended with other complex polymers, mediating interfacial interactions while still maintaining a degree of miscibility in similar, non-surfactant polymers.

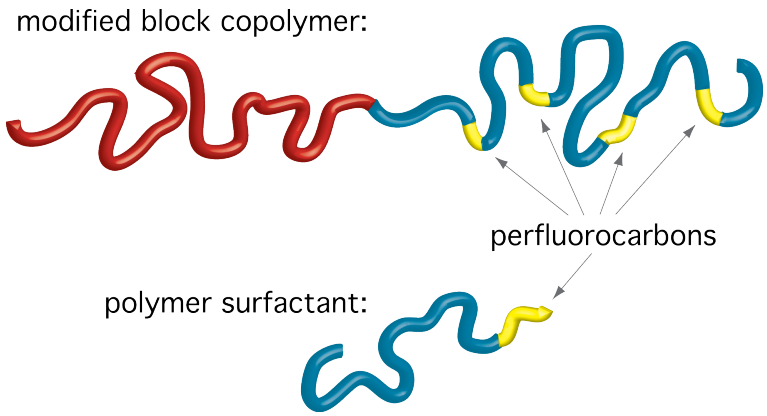

Figure 1.8: Architectural strategies for incorporating perfluorocarbon-functional moieties into block copolymers through copolymerization (top) and end functionalization (bottom).

Perfluorocarbons typically have a low surface energy relative to conventional non-fluorinated polymers. As a result, their covalent attachment to a polymer enhances its propensity to segregate to the surface, deeming such perfluorocarbon-functional moieties as “surface active”. This surface activity has been studied in a

number of polymer systems and exploited in applications for antifouling coatings, organic electronics, and block copolymer lithography.

By using controlled polymerization, accurate perfluorocarbon incorporation can be used to precisely tune surface energy. The low surface energy of perfluorocarbons relative to most polymers is advantageous as small amounts of additive will be needed to induce change and the original structure of the polymer will not be compromised.

To fully comprehend how perfluorocarbon incorporation influences the surface of a polymer, characterization techniques sensitive to the surface must be used to determine structure and composition. Surface analysis is centered around X-ray photoelectron spectroscopy (XPS).

Chapter 2

Experimental Section

During processing, the interaction of a polymer film with a free surface affects its final and surface composition. A strategy to control this interaction and hence tailor the final surface composition of a polymer film is to introduce low surface energy moieties to the system.

The interactions of the end functional polymer will be investigated in solution using dynamic light scattering. The surface characteristics of the polymer blend will be characterized by atomic force microscopy, water contact angle analysis and XPS.
Our goal is control the surface composition of perfluorocarbons and PEO on the surface. Basically what we want is a mixture of perfluorocarbon chains and PEO.

Only PEO does not work well and only perfluorocarbons does not work well either. But the combination of both work better.
PEO is required to inhibit protein adsorption which is the first step in many of the foulants attaching to the surface, and perfluorocarbons give a low surface energy material that helps with the fouling release.

My role was to characterize different samples with different surface compositions and understand wich receipt was able to give us the best compromise between antifouling and fouling release properties.

Dynamic Light Scattering

Dynamic Light Scattering is also known as Photon Correlation Spectroscopy. This technique is one of the most popular methods used to determine the size of particles. Shining a monochromatic light beam, such as a laser, onto a solution with spherical particles in Brownian motion causes a Doppler Shift when the light hits the moving particle, changing the wavelength of the incoming light. This change is related to the size of the particle. It is possible to compute the sphere size distribution and give a description of the particle's motion in the medium, measuring the diffusion coefficient of the particle and using the autocorrelation function.

This method has several advantages: first of all the experiment duration is short and it is almost all automatized so that for routine measurements an extensive experience is not required. Moreover, this method has modest development costs. Another advantage of using dynamic scattering is the possibility to analyze samples containing broad distributions of species of widely differing molecular masses and to detect very small amounts of the higher mass species (<0.01% in many cases).
Behind the theory of this instrument, there are two fundamental assumptions. First is that the particles are in Brownian motion (also called "random walk") and so the distance between the scatters in the solution is constantly changing with time; the second condition is that the beads used in the experiment, are spherical particles with a diameter small compared to the molecular dimensions. Therefore is possible to apply some mathematical relations.

Basically this instrument is composed by a laser, which hits the solution contained in a quartz cuvette (quartz because it is transparent at the laser wavelength used). The light is scattered and detected by a photomultiplier that transform a variation of intensity into a variation of voltage. Two collimating lets are usually used; one after the laser source and the other one just before the photomultiplier. The use of both the collimating lenses is essential in this experiment: the first lens allows us

to focus the beam into the cell, so that the area that we will hit is far enough from the side of the cell. The second lens is used to get an amount of scattered light that is neither too much nor insufficient. The photomultiplier is positioned at a scattering angle of 90 degrees; indeed for this scattering angle it is possible to neglect the nonlinearity of the line width with the scattering angle. After the photomultiplier, the signal is immediately preamplified and then sent to the computer where the voltage is elaborate.

With the controlled parameters of an experiment, it is possible with a light scattering measurement to retrieve the molar mass (M), size (Rh, Hydrodynamic radius), second virial coefficient (A_2), and translation diffusion coefficient (D_T) of a solute solution. All these properties can be measured in solution in a non-invasive manner.

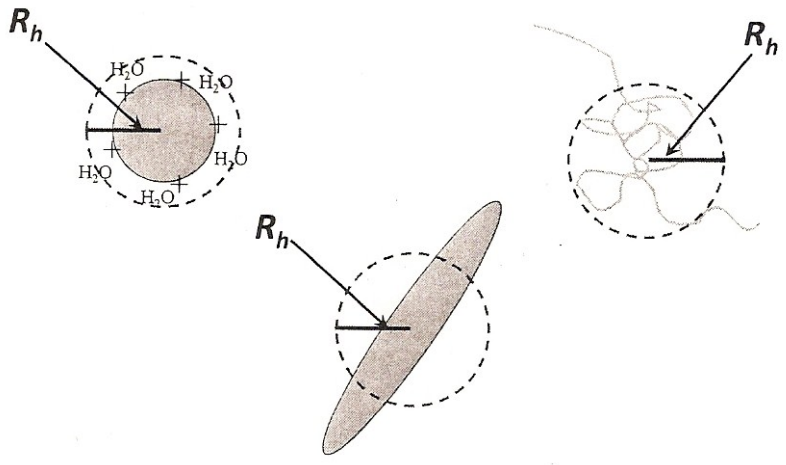

Figure 2.1: Example of Rh and molecular dimensions.

One can still define the hydrodynamic radius as the equivalent spherical radius; i.e. the radius of a sphere with the same translational diffusion constant, but it is no longer simply related to the size.

Depending on the type of experiment, a light scattering measurement retrieves different aspects of the above mentioned properties. For Example, in an

unfractionated sample, or a batch measurement, the measure molar mass is average over the weight distribution of the sample, while the size determined in such a measurement is an average over the radius squared. For fractionated sample, the non-averaged mass and size distributions can be obtained, and from this, information about conformation can be determined.

In the lab we can control the conditions to retrieve detailed information about light scattering. We can choose the wavelength (l), polarization, and intensity (I_i) of the incident light. The size of the laser beam and the field of view of the detector define a scattering volume. We can detect the scattering light (I_s) from this volume as a function of angle (theta) and polarization.

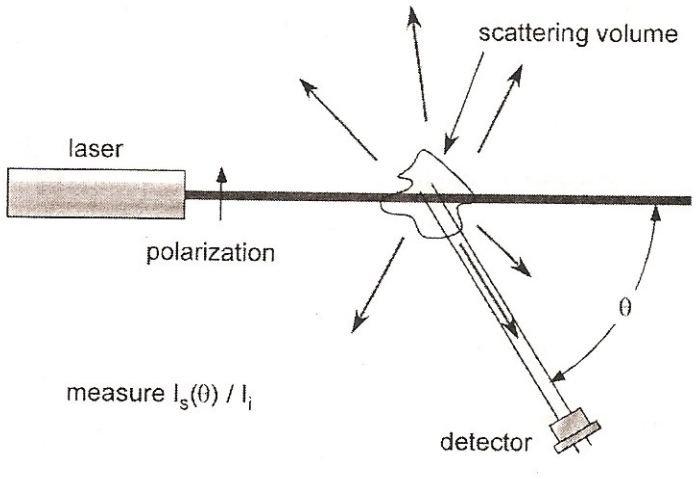

Figure 2.2: DLS set up scheme.

AFM

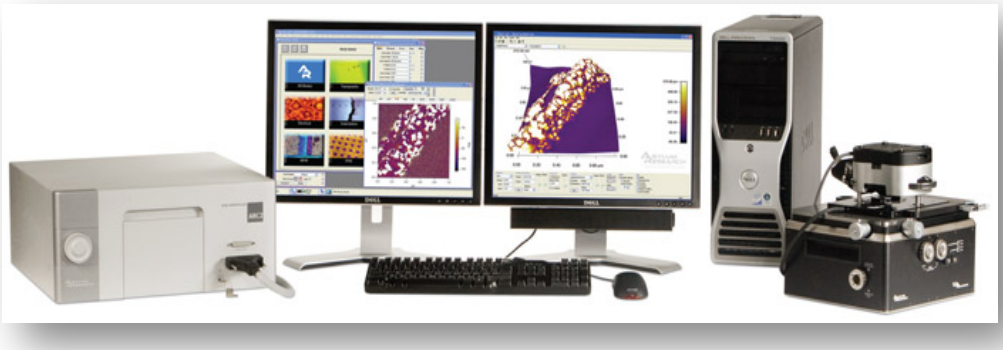

Figure 2.3: AFM equipment.

The most used technique to study block copolymer film morphologies is the scanning probe microscopy (SPM) method referred to hereafter as atomic force microscopy (AFM).

This is a relatively inexpensive lab-based technique that allows imaging of the surface structure. The usual method applied in the case of polymer films is called tapping mode AFM, whereby a sharp tip (usually a silicon or silicon nitride crystal) is oscillated just above the surface of a sample. The tip tracks the topography of the surface and its oscillation frequency is changed by the presence of relatively harder or softer features at the surface, giving rise to so called phase contrast images.

Most AFM measurements are performed on films cast onto flat wafers such as silicon or mica, and are performed in air at room temperature. It is important to consider that buried structures such as cylindrical domains may lead to apparent surface topography in tapping mode AFM due to variations in tip indentation, resulting from stiffness variations.

This was studied in particular via analysis of AFM indentation–distance curves for a PS cylinder-forming PS–PMMA triblock thin film.

Changes in height and phase contrast could be attributed to the crossover between regimes where attractive and repulsive forces dominate the tip-sample interaction. Variable temperature AFM has also been applied to study thermal phase transitions in block copolymer systems.

Figure 2.4: MFP-3D standard atomic force microscope (Asylum Research, Santa Barbara, CA)

Because the atomic force microscope relies on the forces between the tip and sample, knowing these forces is important for proper imaging. The force is not measured directly, but calculated by measuring the deflection of the lever, and knowing the stiffness of the cantilever.

Hook's law gives F = -kz, where F is the force, k is the stiffness of the lever, and z is the distance the lever is bent. In the chart below different force regimes are shown. The distance of the probe from the sample regulates the regime transition.

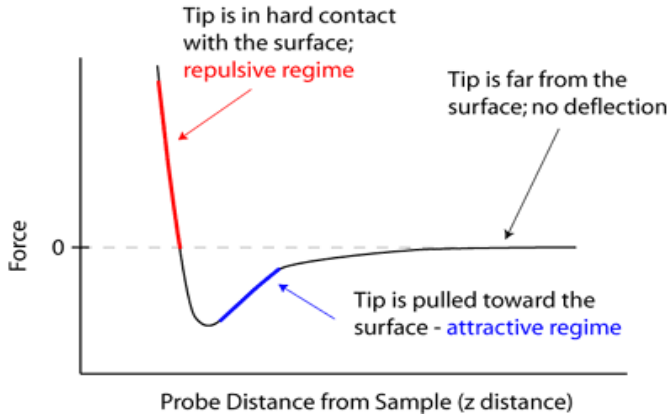

Figure 2.5: Repulsive and attractive regime in AFM set up.

In this figure the interaction forces are sketched as the probe approaches and contacts the surface, with distance increasing to the right. At large separations there are no net forces acting between the probe and the sample surface. As probe and surface approach each other, attractive van der Waals interactions begin to pull the probe towards the surface. As contact is made, the net interaction becomes repulsive as electron shells in atoms in the opposing surfaces repel each other. In this figure, the repulsive forces are shown as being positive and attractive forces negative.

Because of AFM's versatility, there are many different imaging modes available for the AFM, providing a range of different information about the sample surfaces being examined.

Contact Mode.

The first and foremost mode of operation, contact mode is widely used. As the tip is raster-scanned across the surface, it is deflected as it moves over the surface corrugation. In constant force mode, the tip is constantly adjusted to maintain a constant deflection, and therefore constant height above the surface. It is this adjustment that is displayed as data. However, the ability to track the surface in this manner is limited by the feedback circuit. Sometimes the tip is allowed to scan without this adjustment, and one measures only the deflection. This is useful for

small, highspeed atomic resolution scans, and is known as variable-deflection mode.

Because the tip is in hard contact with the surface, the stiffness of the lever needs to be less that the effective spring constant holding atoms together, which is on the order of 1^{-10} nN/nm. Most contact mode levers have a spring constant of < 1N/m.

Lateral Force Microscopy.

LFM measures frictional forces on a surface. By measuring the "twist" of the cantilever, rather than merely its deflection, one can qualitatively determine areas of higher and lower friction.

Noncontact mode.

Noncontact mode belongs to a family of AC modes, which refers to the use of an oscillating cantilever. A stiff cantilever is oscillated in the attractive regime, meaning that the tip is quite close to the sample, but not touching it (hence, "noncontact"). The forces between the tip and sample are quite low, on the order of pN (10^{-12} N). The detection scheme is based on measuring changes to the resonant frequency or amplitude of the cantilever.

Dynamic Force "tapping mode" AFM.

Commonly referred to as "tapping mode" it is also referred to as intermittent-contact or the more general term Dynamic Force Mode (DFM).

A stiff cantilever is oscillated closer to the sample than in noncontact mode. Part of the oscillation extends into the repulsive regime, so the tip intermittently touches or "taps" the surface. Very stiff cantilevers are typically used, as tips can get "stuck" in the water contamination layer.

The advantage of tapping the surface is improved lateral resolution on soft samples. Lateral forces such as drag, common in contact mode, are virtually eliminated. For poorly adsorbed specimens on a substrate surface the advantage is clearly seen.

Force Modulation.

Force modulation refers to a method used to probe properties of materials through sample/tip interactions. The tip (or sample) is oscillated at a high frequency and pushed into the repulsive regime. The slope of the force-distance curve is measured which is correlated to the sample's elasticity. The data can be acquired along with topography, which allows comparison of both height and material properties.

Phase Imaging.

In Phase mode imaging, the phase shift of the oscillating cantilever relative to the driving signal is measured. This phase shift can be correlated with specific material properties that effect the tip/sample interaction. The phase shift can be used to differentiate areas on a sample with such differing properties as friction, adhesion, and viscoelasticity. The techniques is used simultaneously with DFM mode, so topography can be measured as well.

Water Contact Angle

The contact angle (θ) is the angle that a small drop of liquid (pure water in our case) makes in contact with the surface or interface of another phase, usually a solid. The equipment is showed in picture.

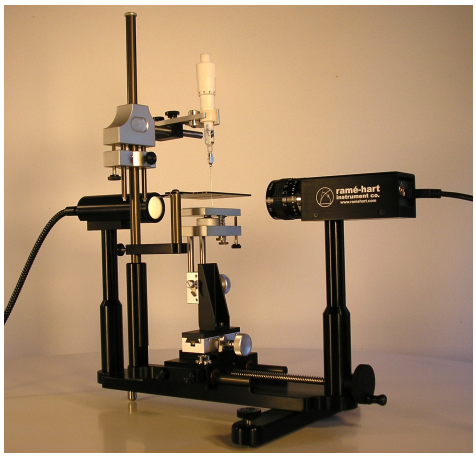

Figure 2.6: Water contact angle experimental equipment.

Water contact angle measurement is the most common method for determining a material's wettability, and the sessile drop approach is the most frequently used.

When the water drop is in contact with the polymer film, it tends to assume different shapes. The flatter is its shape on the surface, the higher is the solid surface tension. We can have an idea of the wettability of the surface based on the angle that the water drop makes with the surface.

In order to assess the wettability of the surface of the polymer films, measurements of advanced and receded contact angles with water as the wetting liquid were carried out as a function of % of AGE.

Introduction of the longer tails resulted in higher contact angles. This was indicative of a relatively high hydrophobicity of the polymer film surfaces

Spectroscopic surface analysis

In order to determine the segregation of chemical moieties to the surface of a polymer film, characterization techniques must be used that are sensitive to only the surface of a polymer film.

A techniques that satisfy this condition and is widely used in this work is X-ray photoelectron spectroscopy (XPS). This technique is performed in ultra high vacuum conditions and make use of X-ray irradiation to generate photoelectrons.

In this techniques the probing depth is limited to $\sim 0 - 10$ nm from the film surface due to the short inelastic mean free path of photoelectrons in carbonaceous media ejected during XPS.

X-ray photoelectron spectroscopy

XPS is a quantitative technique that is capable of determining elemental composition and chemical state at a surface. An X-ray source, such as an aluminum anode, generates monochromatic aluminum Kα X-rays of a known wavelength that are directed toward a sample surface. These photons are sufficient in energy to eject electrons from an occupied orbital into vacuum (Figure 2.7) where the kinetic energy of the ejected photoelectrons is analyzed by a detector at an angle from the surface normal, φ, that can be adjusted.

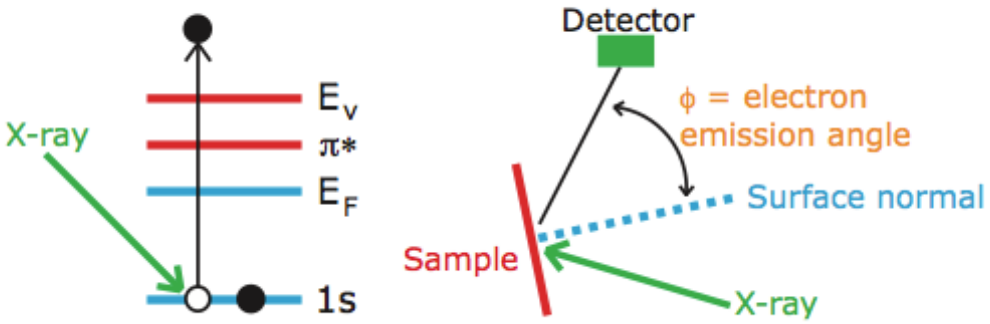

Figure 2.7: Energy transfer from a bonding orbital (left). An X-ray of known energy ejects a photoelectron into vacuum. The kinetic energy of the photoelectron is analyzed by a detector at an angle from the surface normal (right).

By quantifying the energy of the ejected photoelectrons, the binding energy, *EBE,* of the electron can be calculated by

$$h\nu = EKE + EBE + \Phi$$

where $h\nu$ is the energy of the incoming X-ray irradiation, *EKE* is the kinetic energy of the ejected photoelectrons, and Φ is the work function of the spectrometer. Electron binding energies are unique to the atom they are associated with and to the chemical state the atom is in.

A range of spectral databases can then be used to determine the chemical composition and states that exist at the surface of a sample.

Due to the short inelastic mean free path (IMFP) of photoelectrons, XPS produces data that is only representative of the top ~ 10 nm of a surface.

If the IMFP of a photoelectron, passing through a certain medium is known, it is possible to determine information about the depth profile at the surface using angle resolved XPS (ARXPS). Through sample rotation it is possible to vary φ and control the effective sampling depth, λ∗, by

$$\lambda* = \lambda \cos(\varphi)$$

where λ is the IMFP of a photoelectron of a given energy traveling through a defined medium. λ can be experimentally determined or calculated through the use of a database. (Figure 2.8) shows how with increasing φ the effective sampling depth is reduced, making the XPS measurement more surface sensitive.

If the surface contains an overlayer of that differs in elemental composition from an underlayer, it possible to calculate the thickness, *t* of the overlayer using the following equation:

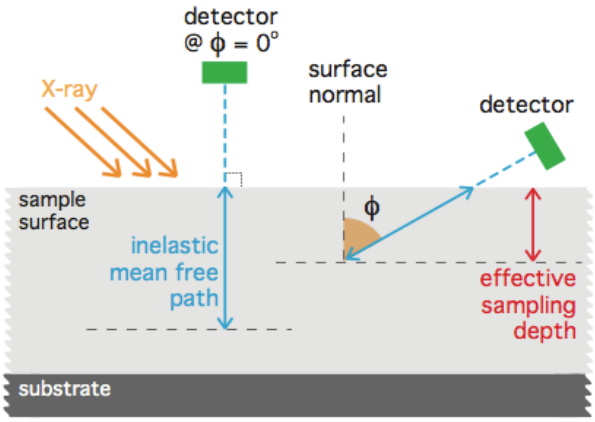

Figure 2.8: Schematic depicting concept of angle resolved XPS. By increasing the angle between the surface normal and detector, ϕ, the effective sampling depth is reduced, making the measurement more surface sensitive.

$$\frac{t}{\lambda \cos(\phi)} = \ln\left[1 + \left(\frac{I_o}{I_u}\right)\frac{\rho_u s_u}{\rho_o s_o}\right]$$

where I_o and I_u are the relative intensities of photoelectrons emitted from elements distinct to the overlayer and underlayer respectively, ρ_o and ρ_u are their corresponding atom densities, and s_o and s_u are the relative sensitivity factors of the analyzer detector to the elemental signals. ARXPS measurements can be used to determine how well defined the overlayer is by plotting $\ln[1+(I_o/I_u)(\rho_u s_u/\rho_o s_o)]$ *vs* $\cos(\varphi)$, where a straight line through the origin would signify a uniform overlayer with a discrete interface.

One disadvantage to this method is that typically values for s_o and s_u are machine specific and must be calibrated regularly using material standards. This results in a less accurate calculation of film thickness. However, in many situations, due to the bonding environment of atoms, has made it possible to avoid the use of relative sensitivity factors by focusing on one elemental peak. This is possible because photoelectrons ejected from orbitals of atoms that are bonded to more electronegative atoms have a higher binding energy. For the analysis of organic polymer surfaces, differences in the electronegativity of functional groups make it possible to determine the chemical composition by focusing on the carbon 1s orbital electrons.

Using XPS to analyze the surface of a highly functional block copolymer exemplifies the applicability of the technique. Scheme depicts a surfactant functionalized triblock copolymer as a potential anti-biofouling coating. The polymer was synthesized from a polystyrene-*block-poly(ethylene-stat-butylene)-block-polyisoprene* precursor *via* post modification of epoxides created from the polyisoprene block. The functional group, is a linear molecule consisting of a few ethylene oxide units and is terminated by a $-(CF_2)_9CF_3$ chain. The low surface energy perfluoro-carbons brings the groups to the surface of the polymer film

after processing, displaying an increased concentration of carbons bonded to fluorine and oxigen.

By acquiring a high resolution scan of the carbon 1s region, it is possible to accurately quantify the amount of the groups and other functionalities at the surface, and develop a depth profile for each chemical moiety.

Figure 2.9 depicts the XPS spectra of the functional polymer with a graphical representation of the experimental geometry above the plot. The data were acquired at $\varphi = 0^{\circ}$ and at $\varphi = 75^{\circ}$, thereby decreasing the effective IMFP and increasing the surface sensitivity.

The spectra contain five peaks that, in order of increasing binding energy, are due to carbon 1s photoelectrons emitted from carbons bonded in the following environments: C–C/C=C/C–H (285 eV), C–O (286.5 eV), C–CF2 (CH2 next to CF2) (289 eV), CF2 (292 eV) and CF3 (294 eV).

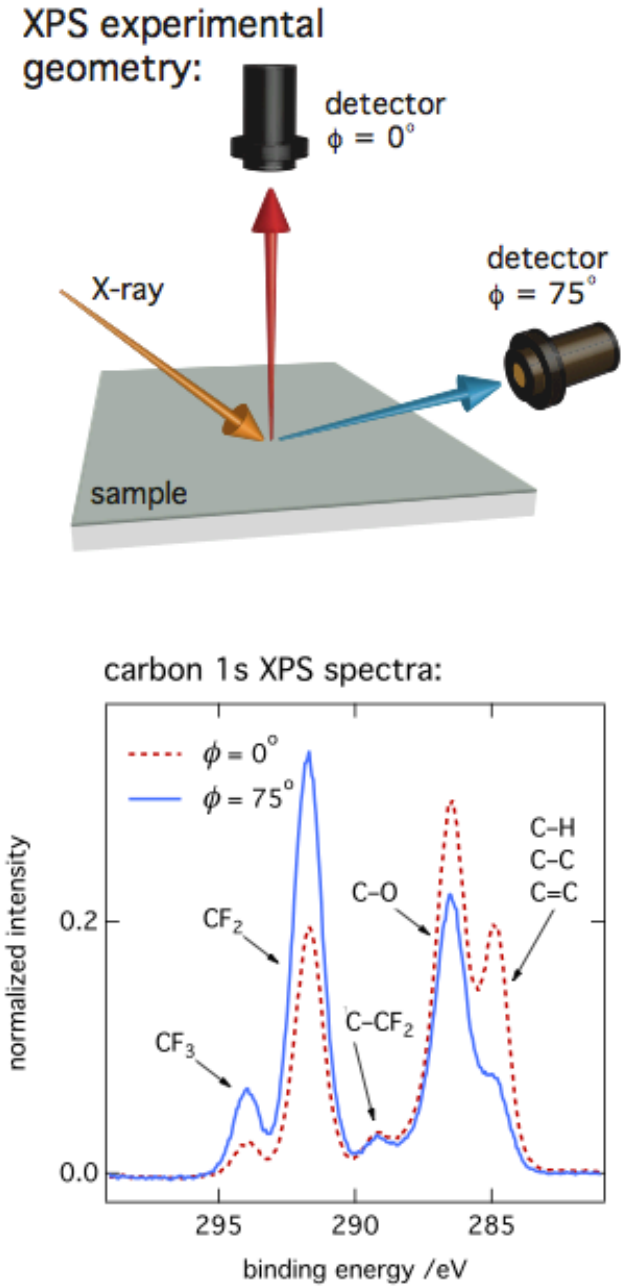

Figure 2.9: XPS spectra of ZonylR functional triblock depicted in scheme recorded at a ϕ of 0 and 75 (bottom). Experimental geometry depicting angles of ϕ is illustrated above.

Each peak can be fit to a Gaussian function to determine the relative surface concentration of each chemical state on the surface and differences in peak intensities with changing φ denote a depth profile of each state.

The spectra in figure 2.9 show an increased concentration of CF_2 and CF_3 and a decreased concentration of C–C/C=C/C–H and C–O as φ is increased to 75°. This can be interpreted as a segregation of the perfluorocarbon portion of the group to the surface while the ether carbons and polymer backbone remain underneath.

It is the quantitative surface composition and depth profiling information XPS can render that makes the technique a powerful tool in characterizing a material surface.

Preparation of the solutions

The goal in this case was to investigate the size distribution profile of small particles in suspension or polymers in solution and observe the presence of aggregation or not. The model system used is end-functional poly(2-vinylpyridine) in a blend with poly(2-vinylpyridine) (P2VP). The polymer has been diluted in different solvents; we wanted to see if different solvent could influence the distribution of the polymer in solutions. It has been used two different solvents, Tetrahydrofuran (THF) and Pyridine.

The desire solution concentration was 3wt%, so the solution was composed of 0,030 g of polymer and 10 ml of solvent. The quantity of polymer has been measured with a scientific balance and in every measurement an error of ± 0,0010 mg had to be considered.

To assure the purity of the solvent, it has been filtered with a 0,45 μm PTFE filter.

The polymers analysed were P2VP and P2VP$(C_6F_{13})_4$.

We used the Gel Permeation Chromatography (GPC) to determinate the molecular weight distribution and so verify the quality of the polymer before analysing it with the DLS. The polymer for the GPC has been diluted in chloroform.

The gel permeation chromatography (GPC) is also known as size exclusion chromatography, and a chromatographic technique in which the molecules of the analyzed sample are separated according to their different sizes.

This technique is usually applied to macromolecules, such as biological or synthetic polymer.
GPC has stationary phase and consists of a porous polymer gel, with poresizes.
When the eluent flows through the column, the smaller molecules can enter in all the pores of the stationary phase, while larger ones are excluded. The larger is the molecule, the lower are the number of pores in which it can enter and therefore the path through the column is shorter and the elution is faster.
The smaller is a molecule, the greater are the number of pores in which it enters along the path, and this obviously takes more elution time.

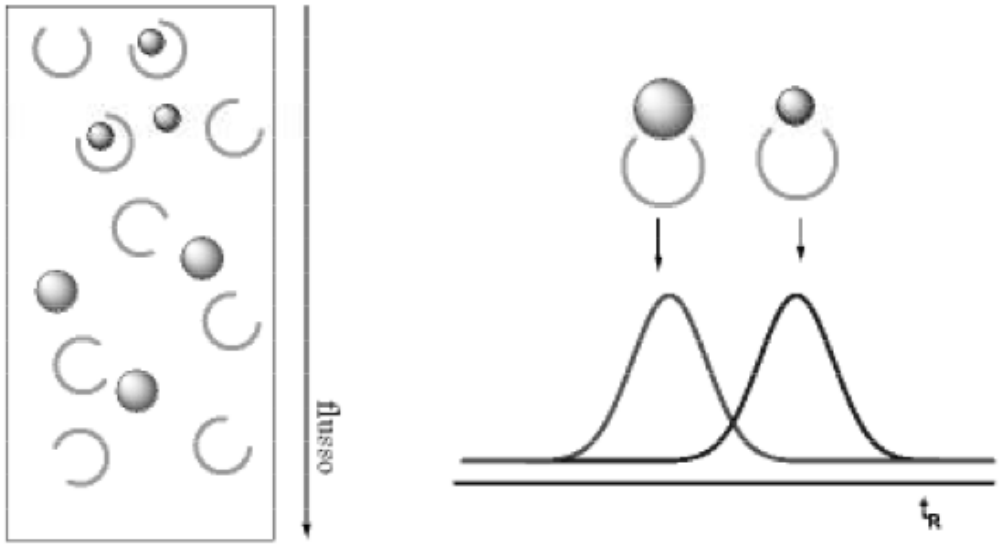

Figure 2.10: GPC size distribution scheme.

The GPC profile obtained is represented in the following graph:

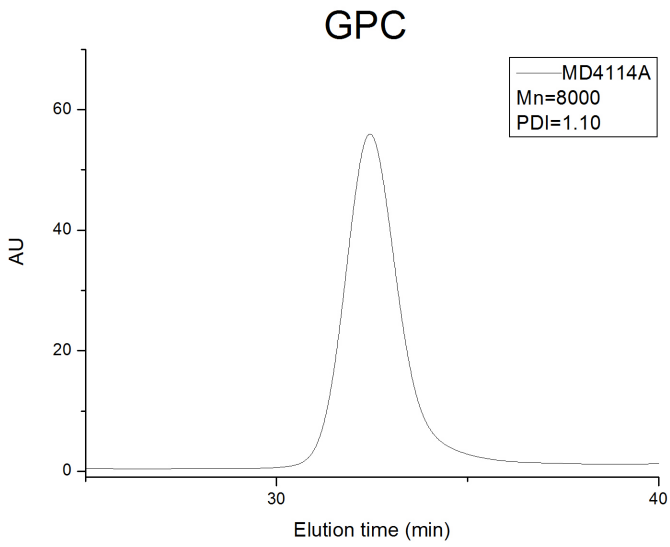

Figure 2.11: P2VP GPC profile.

In the DLS analysis, we dropped 4/5 drops of solution in a quartz cuvette. We also did a measurement of pure solvent as a reference (blank).

The parameters used in the DLS instruments analysis were: number of acquisitions 10 with 10 seconds of time between each acquisition. The measurement has been repeated with also 5 seconds between each acquisition.

Spin Coating techinique

The step consists in preparing the samples using a silica substrate.
For convenience (saving polymer in solution and for the equipment settings) we cut the monocrystal silica wafer in small squares of max 1 cm side. Cutting the edge of the square was very easy because it was a monocrystal, in fact we just had to follow the crystal direction or cut it in the perpendicular direction. We planned to cut 4 silica squares for each solution.

Before proceed with the deposition of the solution we had to be sure that the silica surface was completely clean. In order to achieved that we treat them with the sonication in different solvents.

We putted the silica tiles in a proper wafer holder; we soaked them in a 200 ml solution of acetone and leave them in the sonicator for 10 min. After that we soaked them in isopropanol first and distilled water then, for both we did the sonication. The process had to be repeated 2 times. After that we dry them with air compressed.

Figure 2.12: Sonicator used to clean the sample.

The second step consists to prepared the solutions. The solvent used for the dilution was dioxane. We wanted a 3wt % solution so we diluted 30 mg of polymer in 1 g of dioxane. We also made some solutions with a content of different polymers (fluorinated and not), one with 100% of P2VP, one 10% P2VP-(C6F13)4 (3 mg) and 90% P2VP (27 mg) and another one 100% P2VP-(C6F13)4, we just wanted to observe how the fluorine arranged once it was deposited on the wafer.

We also wanted to prepared solutions with a fluorinated polymer with different arms, 1 and 2 arms. We kept the same concentration (3wt%) and mixed them in dioxane as well. The proportions were 10% 1 arm (3 mg) and 90% (27 mg) 0 arm for one solution and 10% 2 arm (3 mg) and 90% 0 arm (27 mg) for the other solution.

For the spin coating we used the device in the picture.

Figure 2.13 Spin Coating equipment.

Spin coating is a procedure used to apply uniform thin film to flat substrates. In short, an excess amount of a solution is placed on the substrate, which is then rotated at high speed in order to spread the fluid by centrifugal force.
The solvent used is usually volatile, so it tends to evaporate. The rotation keeps going until the fluid reaches the edge of the tile.
The final thickness of the film depends on the angular speed and the concentration of the polymer in solution and the solvent. So the higher the angular speed, thinner the film.

In the process there are 4 basic steps:

- deposition of the coating fluid onto the wafer or substrate;

We dropped about 2 or 3 drops of solution over the surface. We used a syringe with a 0.45 μm PTFE filter.

- Acceleration of the substrate up to its final, desired, rotation speed;

the rotation speed used was 3000 rpm for 45 seconds.

- Spinning of the substrate at a constant rate; fluid viscous forces dominate the fluid thinning behavior;
- Spinning of the substrate at a constant rate; solvent evaporation dominates the coating thinning behavior.

Once we got the solutions and prepared the samples, the solutions were kept in the refrigerator to prevent and to be sure the polymer in solution did not begin the polymerization.

Annealing

Four samples for each solution were made and 1 sample for solution were annealed. The samples have been in the oven for 2 days at 170°C. The highest temperature has been reached gradually with a proper temperature ramp. The plateau is called soaking time and it is the time we left the structure to arrange and find an equilibrium. Then the system has been slowly cooled to room temperature.

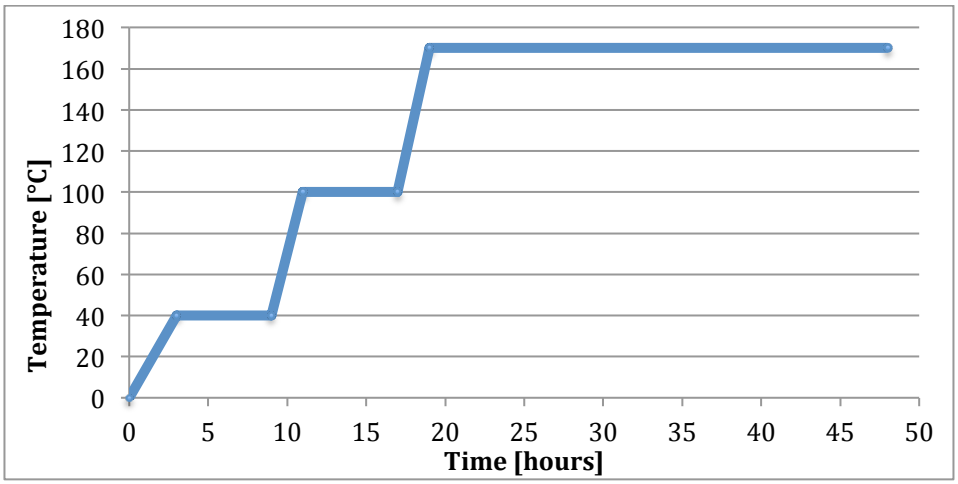

Figure 2.14: Annealing temperature ramp.

All the annealing treatment has been done in vacuum (1.0×10^{-8} Torr) in inert atmosphere (N_2).

Chapter3

Results and Discussions

We have considered two systems. In the first one we consider the study of the P2VP-CF. We examined this molecule in different solvents with the DLS. The factors might affect the polydispersity and the size distributions are the concentration, the number of C_6F_{13} (arms) and the solvent. For this reason besides the polymer in different solvent we also examined polymers with different number of arms. We consider the same concentration for each measure of 3mg/ml. From the measurements with the DLS we obtained the following graphs.

The measures have been done with The DynaPro NanoStar™ from Wyatt Technology.

Figure 3.1: DLS equipment DynaPro NanoStar™ from Wyatt Technology.

THF solvent:

P2VP

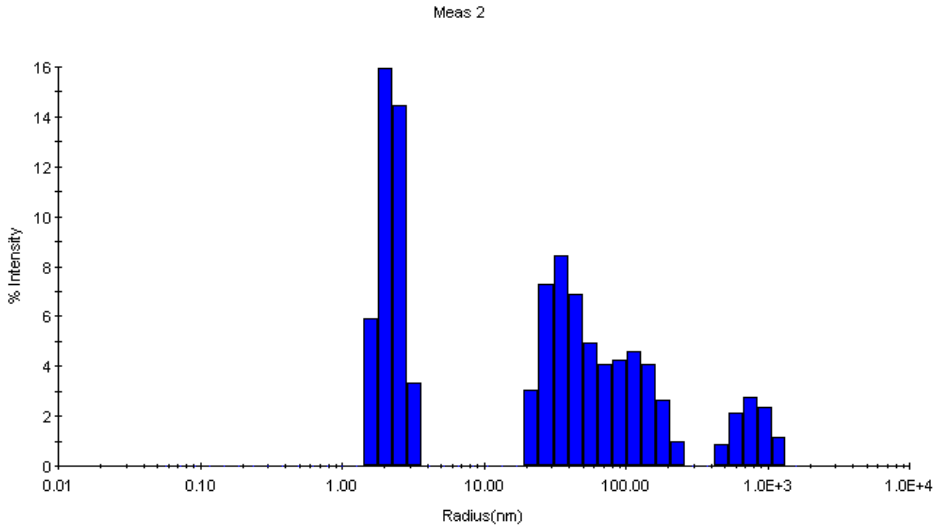

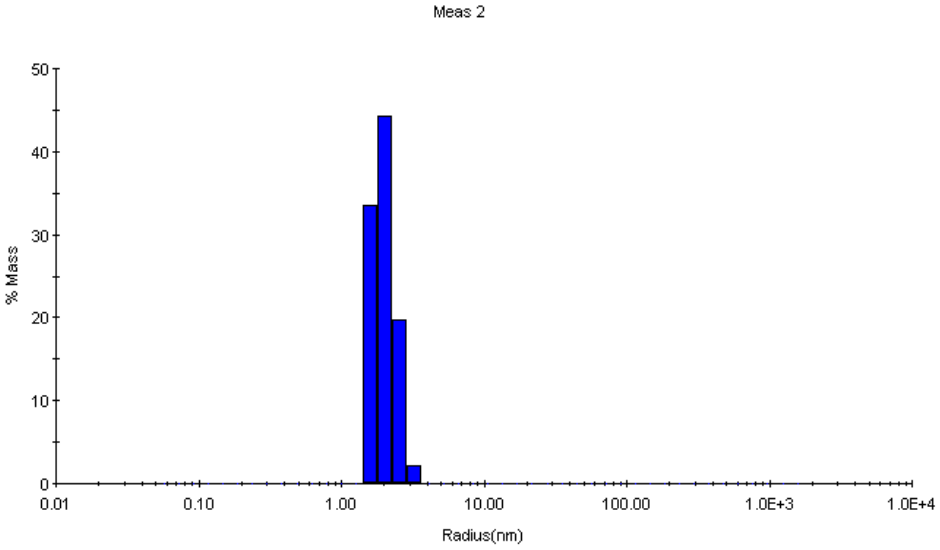

P2VP(C_6F_{13})$_4$

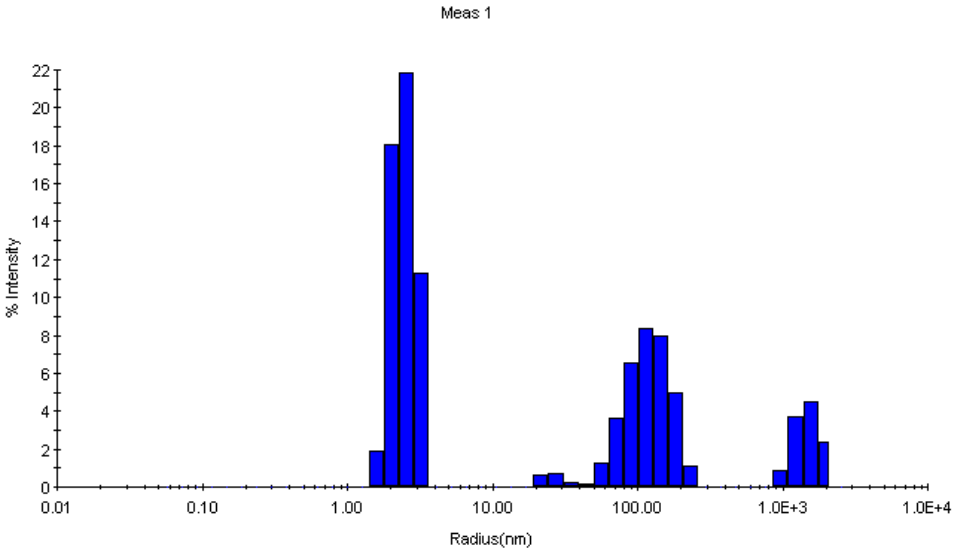
Meas 1
% Intensity
Radius(nm)
0.01
0.10
1.00
10.00
100.00
1.0E+3
1.0E+4

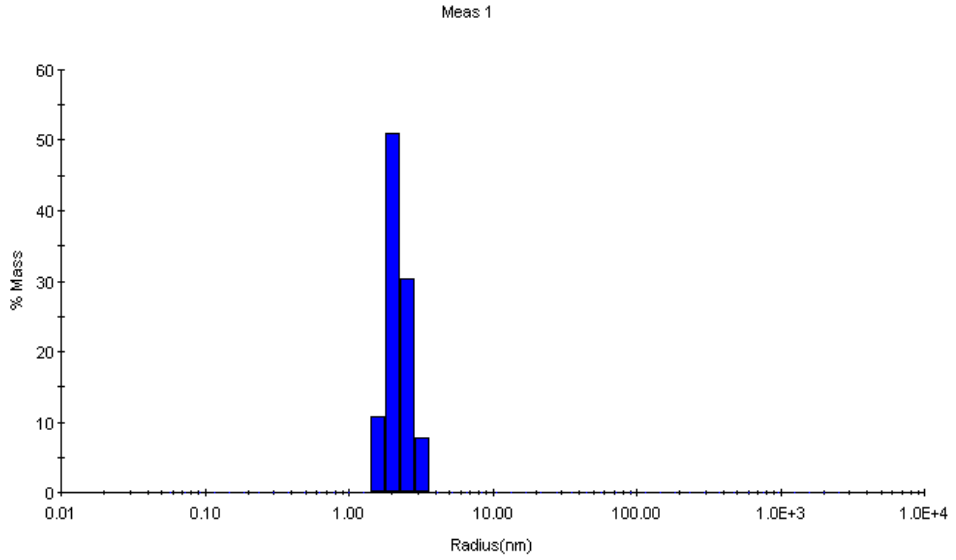
Meas 1
% Mass
Radius(nm)
0.01
0.10
1.00
10.00
100.00
1.0E+3
1.0E+4

P2VP(C_6F_{13})$_8$

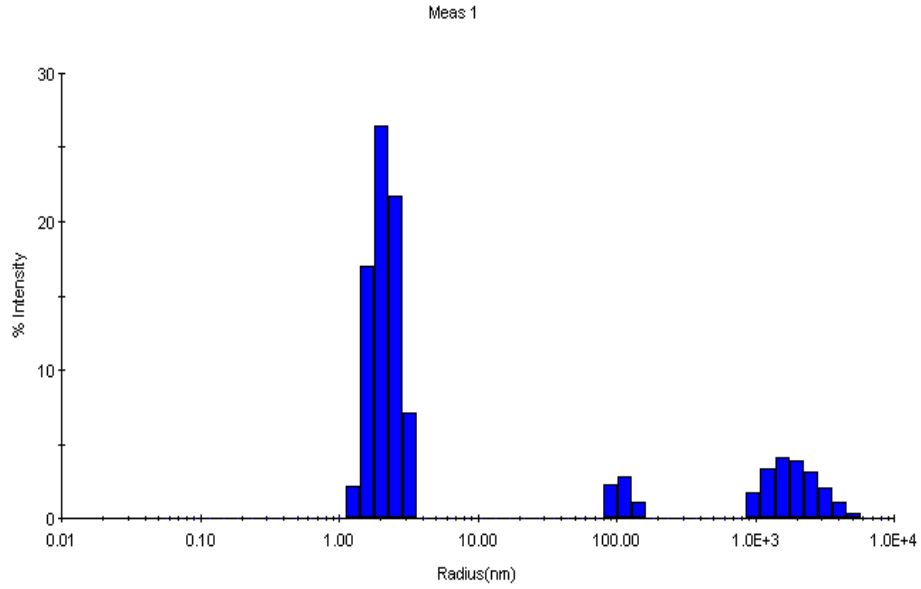
Meas 1
% Intensity
30
20
10
0
0.01
0.10
1.00
10.00
100.00
1.0E+3
1.0E+4
Radius(nm)

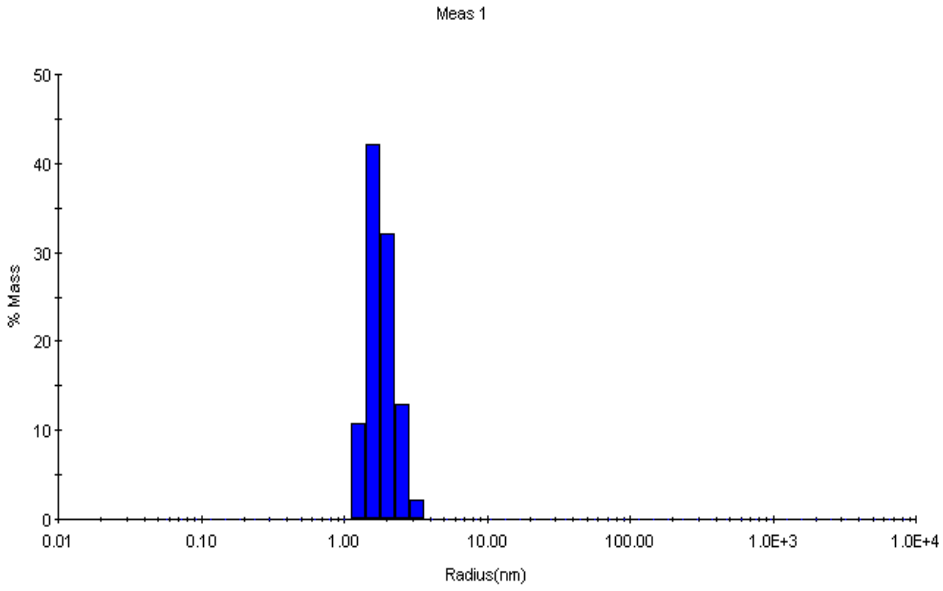
Meas 1
% Mass
50
40
30
20
10
0
0.01
0.10
1.00
10.00
100.00
1.0E+3
1.0E+4
Radius(nm)

$P2VP(C_6F_{13})_{16}$

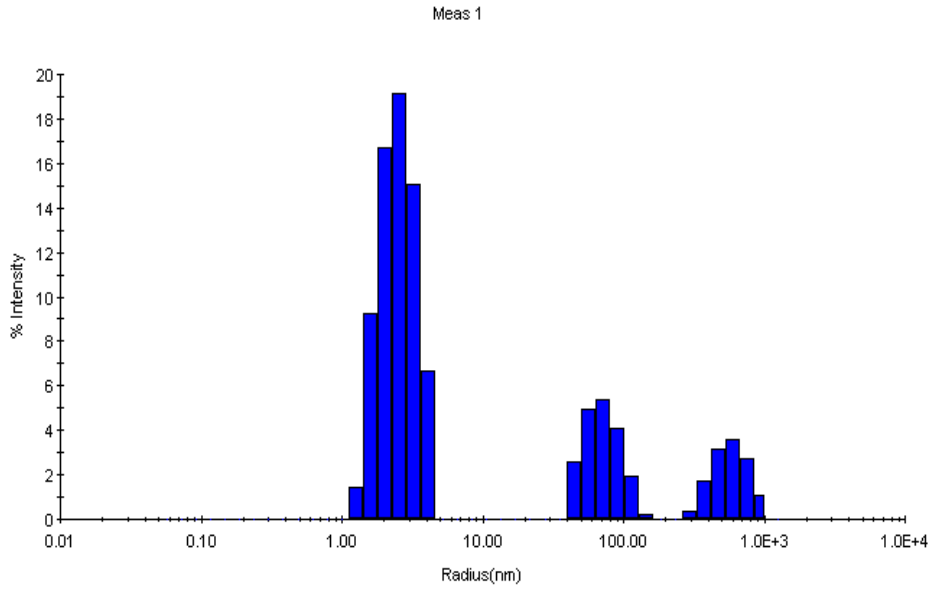

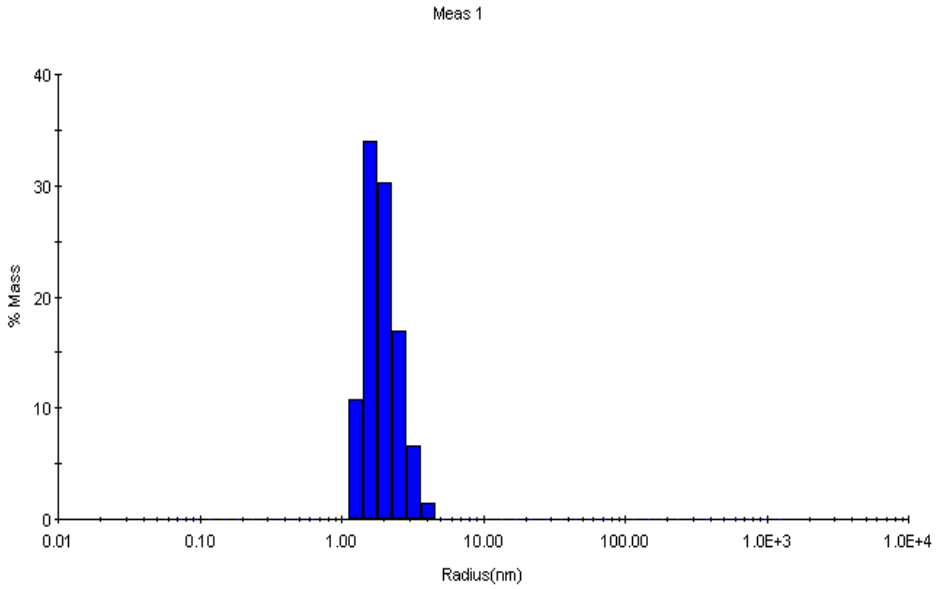

In Pyridina:

P2VP not filtered

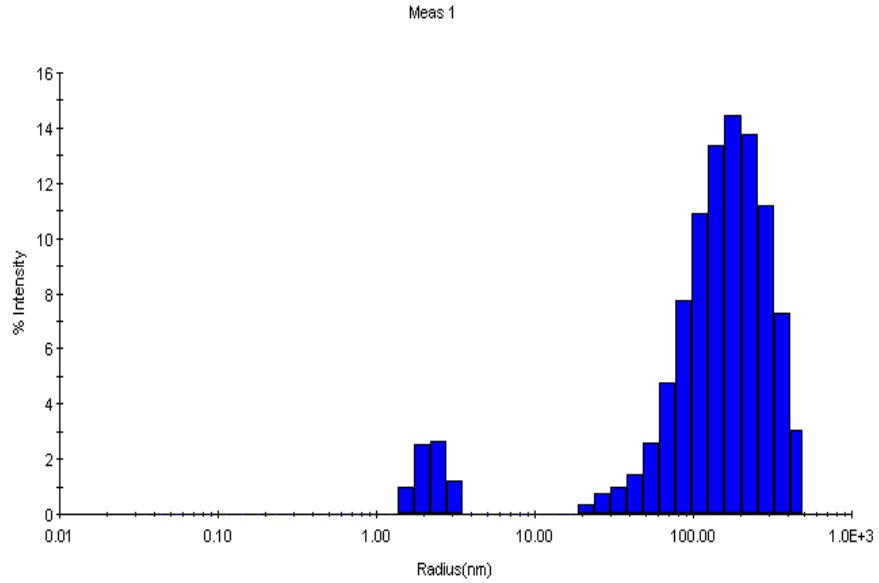

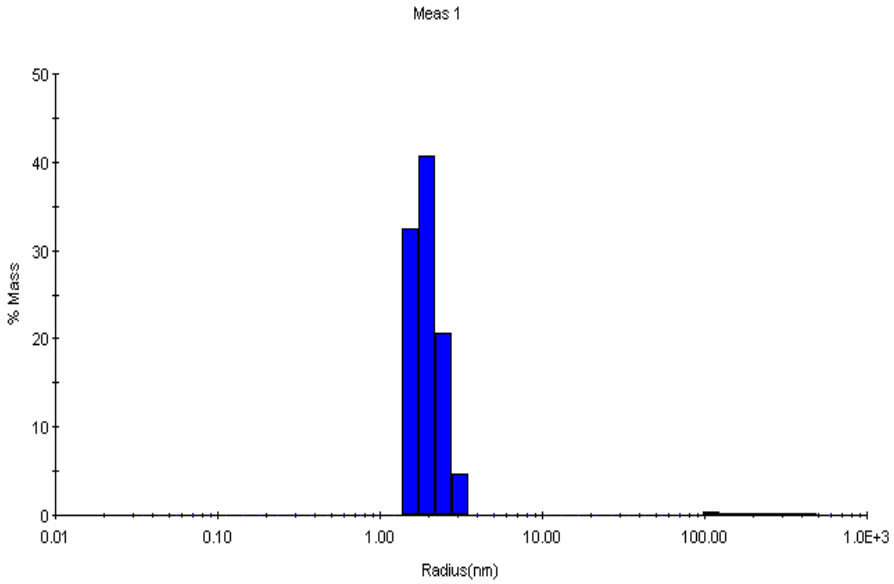

$P2VP(C_6F_{13})_4$

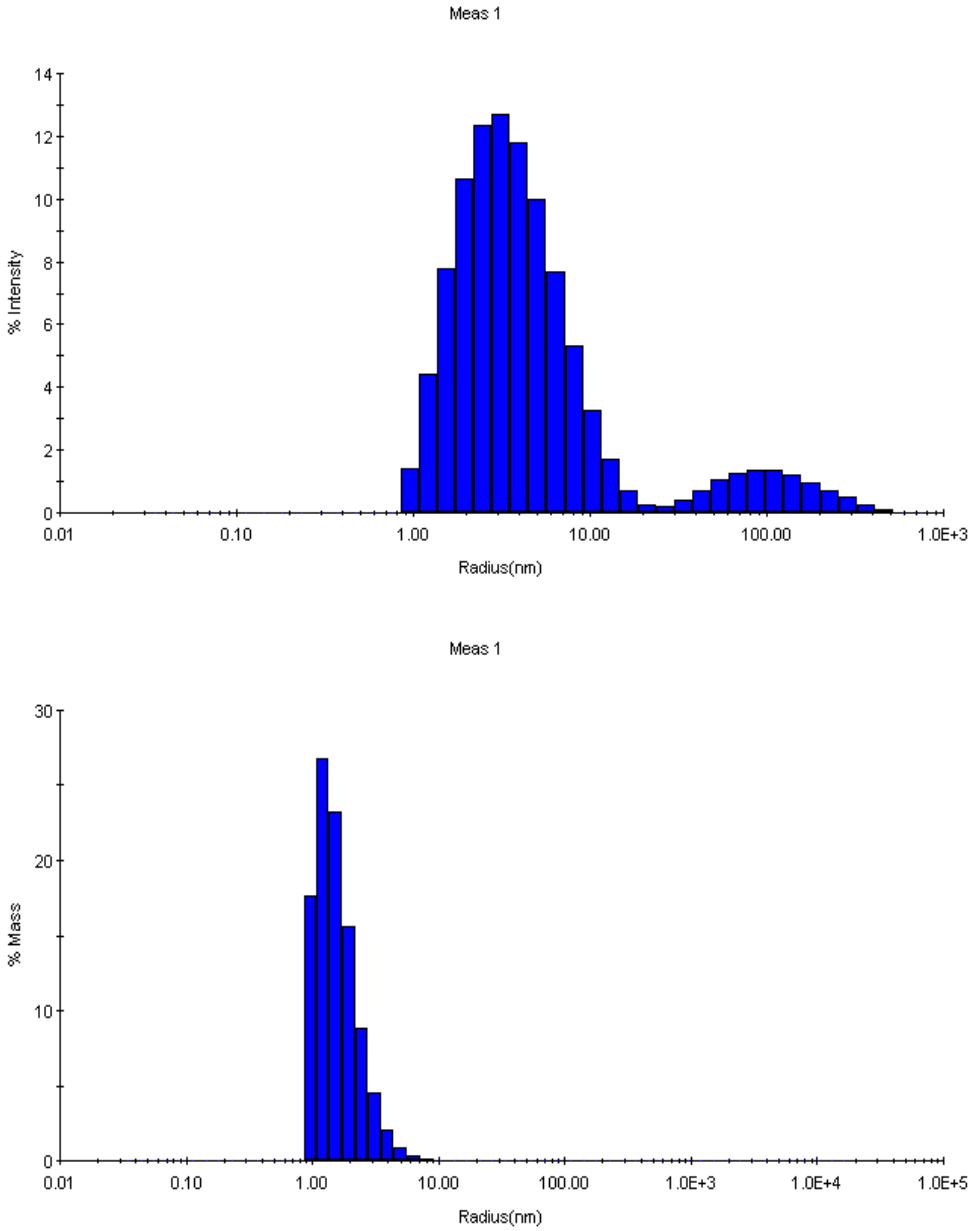

Figure 3.2: DLS histograms of different polymers and different solvents: a) THF solvent, (I) P2VP, (II) $P2VP(C_6F_{13})_4$, (III) $P2VP(C_6F_{13})_8$, (IV) $P2VP(C_6F_{13})_{16}$. b) Pyridine solvent, (I) P2VP not filtered, (II) $P2VP(C_6F_{13})_4$.

Each graph shows intensity vs radius of the particles and mass vs radius.
In these measurements we were interesting to evaluate the size and polydispersity.
For size we refers to the radius of the particle considered as a sphere that moves or diffuses in the solution. To determine this value we looked at the peak of the size distribution. The data are reported in histogram form and the size of the particles are dispersed or spread or allocated among one or more peaks.

The polidispersity is referred to the width of the peak. Polydispesity is a measure of heterogeneity or homogeneity of the species comprising in the population.
In Y we have the % Intensity that is the % of total light scattered, basically it represents the probably of existence of the species. In X axis the particle size in nanometers.

If the graph presents only one peak we can call it monomodal size distribution, its width is the standard deviation of the weighted bin values, what we call polydispersity.
If the histogram presents more than one peak, we can define it a multimodal size distribution, that means we have different size population, e.g. 3 peaks means 3 distinct population in the same solution. In this case we can consider the system heterogeneous.

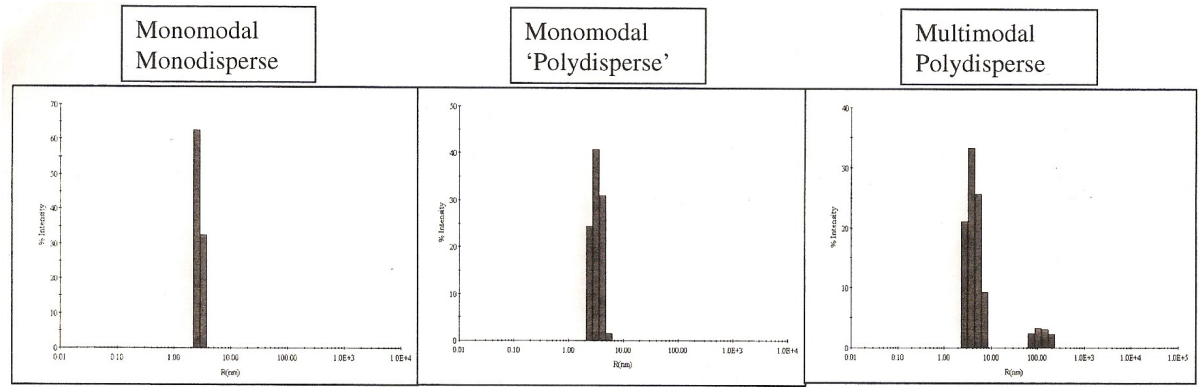

Figure 3.2: examples of monomodal and multimodal size distribution.

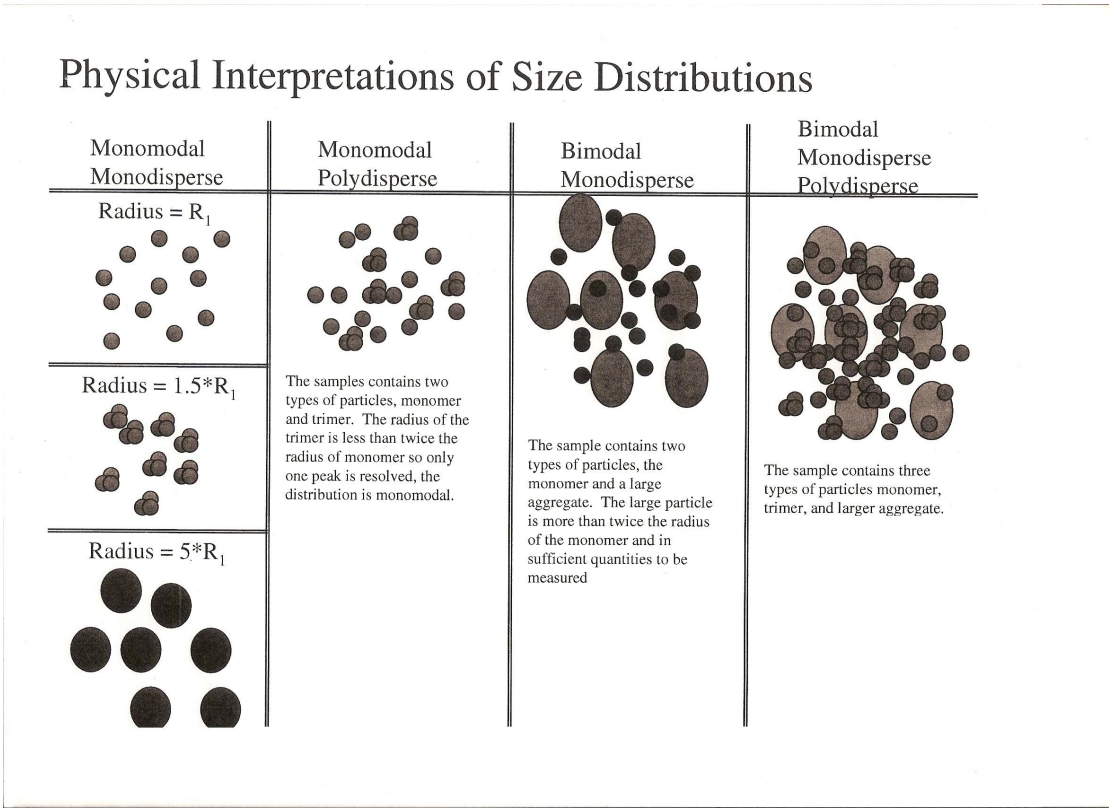

Figure 3.3: Different modes and relative examples of size distribution.

To evaluate the goodness of the data we first have to observe the correlation function of each measurement. Three possible examples of autocorrelation function are reported below.

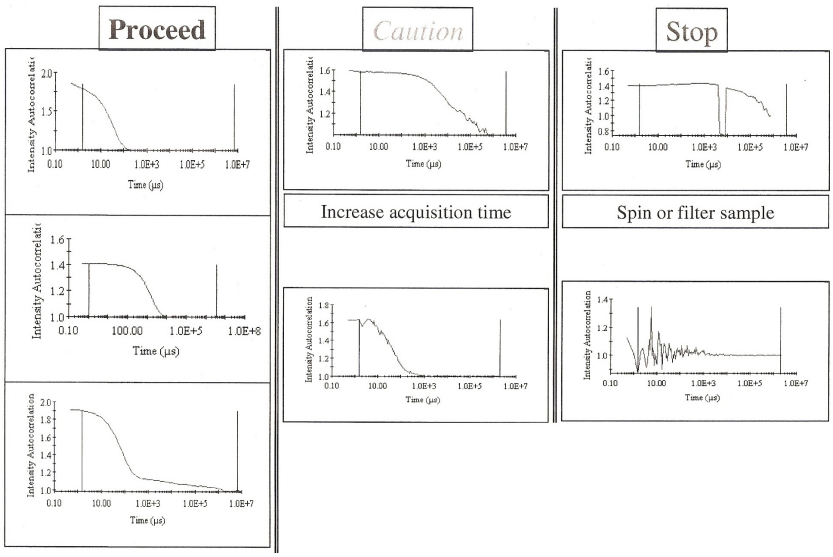

Figure 3.4: Three different types of autocorrelation functions.

In most of all measurements I had a pretty good autocorrelation function, figure 3.4 shows a reference example; we had autocorrelation function similar to first group of graphs in figure. In case of a noisy function like the second graph in the "caution" section, I had to modify some setting conditions like increase acquisition time, increase acquisitions or increase laser power.

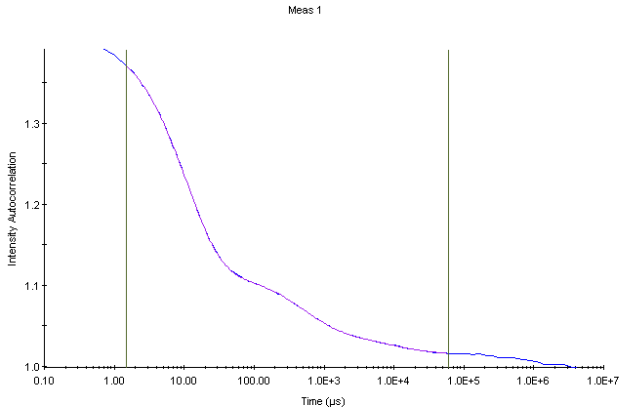

Figure 3.5: Example of autocorrelation function obtained from the experimental data of P2VP$(C_6F_{13})_4$ in THF solvent.

In the data presented, regarding the THF solvent, all the graphs (intensity graph) show a multimodal size distribution due by the presence of at least three peaks in each graph. This means we had different size population. We do not have different species cause we know what we had in solution.

Different populations can be caused by aggregation of smaller molecules. The peaks show a polydispersion (width of each peak). For each population we have monomer of different radius.

We do not see any significant aggregation to prove the existence of micelles.

Fundamental is to make sure that there are no micelles in the solution before we deposit. This is important because if we are forming micelles we are changing the structure of the film when we deposit it with spin coating. This will change the surface structure

AFM

We wanted to analyzed how the P2VP macromolecules with arms and without arms arrange when deposited on substrate, in our case, silica. In particular we were interested to see the behavior of fluorine. For this purpose we looked at the samples with the Atomic Force Microscopy (AFM).
The instrument used was a MFP-3D standard atomic force microscope (Asylum Research, Santa Barbara, CA)

AFM is a very sensitive device that needs to be set properly. Firstly we had to set the tip and once we put the sample to analyze, make sure we had a proper contact between the sample and the tip. The tip had to touch the sample, but neither push to it too much or barely touch it. The result of a bad contact sample/tip gives a noisy signal or can lead to the tip breakage.

The first samples analyzed were the 100% P2VP (0 arms) and the 10% P2VP-$(C_6F_{14})_4$ (4 arms) / 90% P2VP for both the solutions we analyzed the annealed and not annealed samples as well.

100% P2VP (annealed)

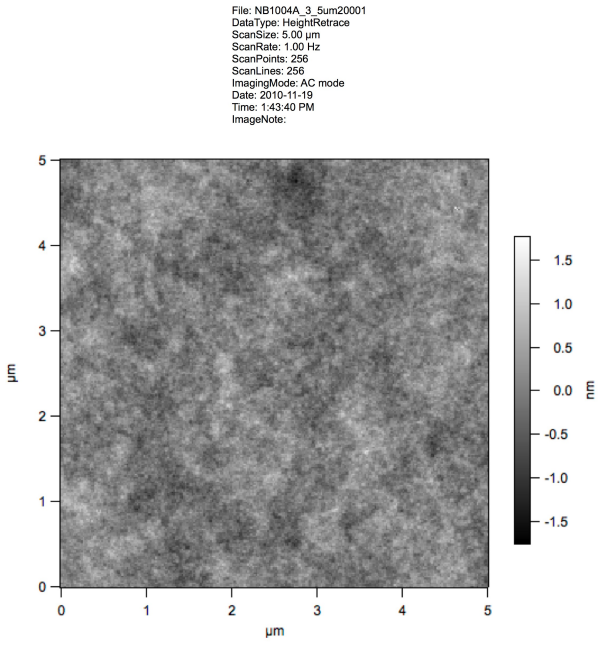

100% P2VP (not annealed)

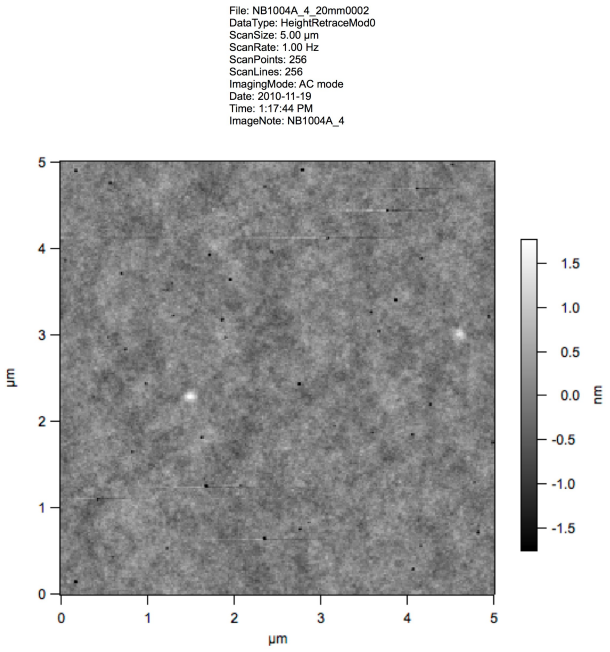

90% P2VP and 10% P2VP-$(C_6F_{14})_4$ (annealed)

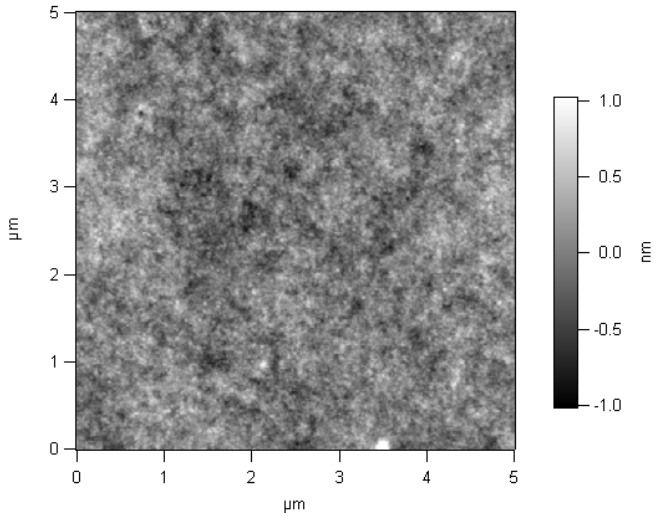

90% P2VP and 10% P2VP-$(C_6F_{14})_4$ (not annealed)

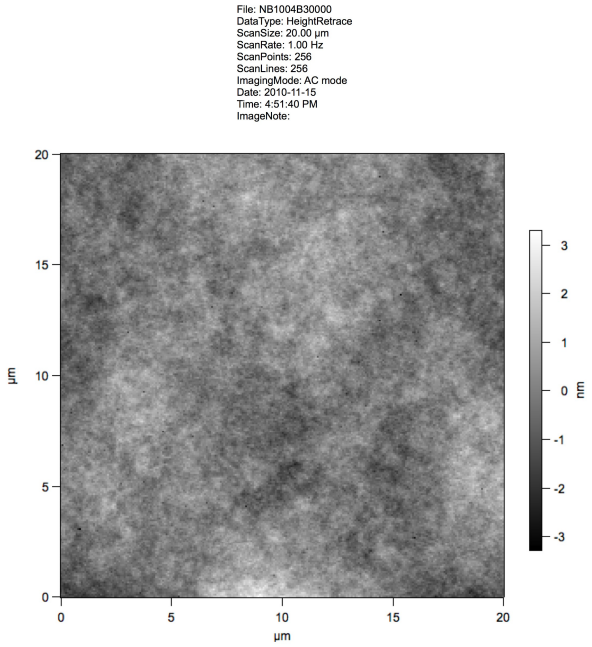

Figure 3.6: AFM images of P2VP annealed/not annealed and P2VP with P2VP-$(C_6F_{14})_4$ annealed/not annealed.

All the images are 5 μm scale. All of them show pretty flat surfaces, the annealed samples have a little bit rougher surfaces. There are not differences between the samples with arms and without arms.

We kept the same solvent (dioxane) and we mixed the 1 arm polymer with the 0 arms (5% and 90% respectively) and also the 2 arms with 0 arms (5% and 90% as well). We thought the reason we did not see anything in the previous images, might be attributed by the steric encumbrance of the macromolecules with 4 arms.

Their arms presented an obstacle to the molecular rearrangement, so we tried to use polymers with less arms (1 and 2 arms) and so less fluorine.

The concentration of the solution was still 3wt%.

5% P2VP(C_6F_{14}) and 95% P2VP (not annealed)

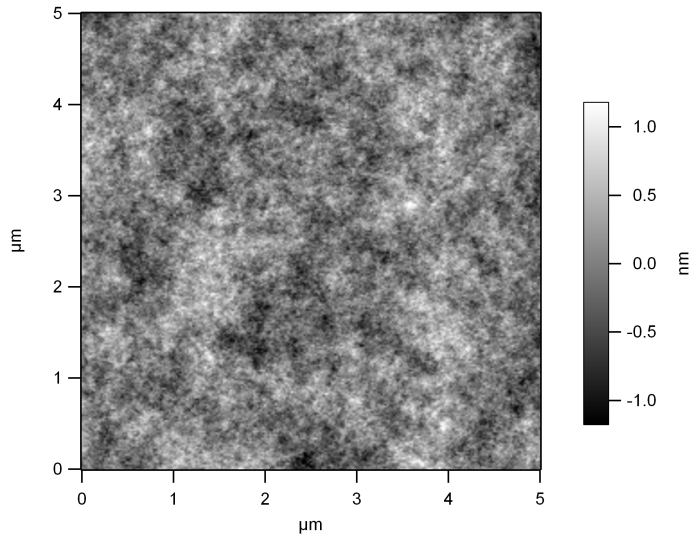

5% P2VP(C_6F_{14}) and 95% P2VP (annealed)

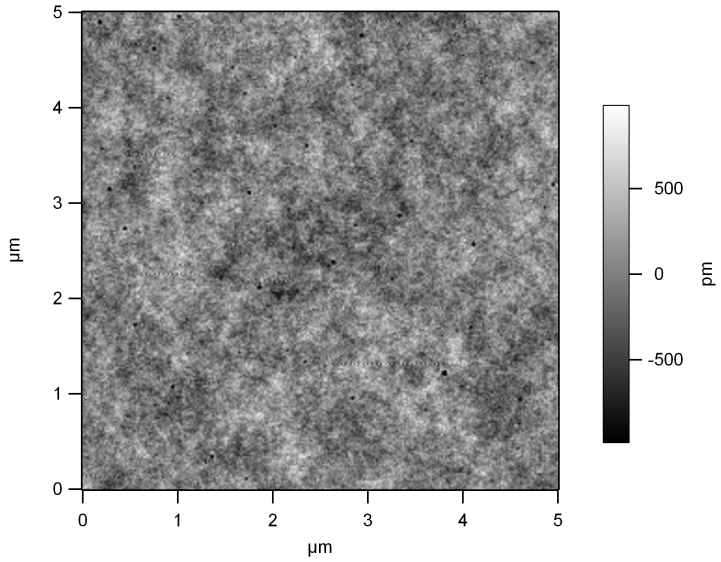

5% P2VP(C_6F_{14})$_2$ and 95% P2VP NB1011B3 (not annealed)

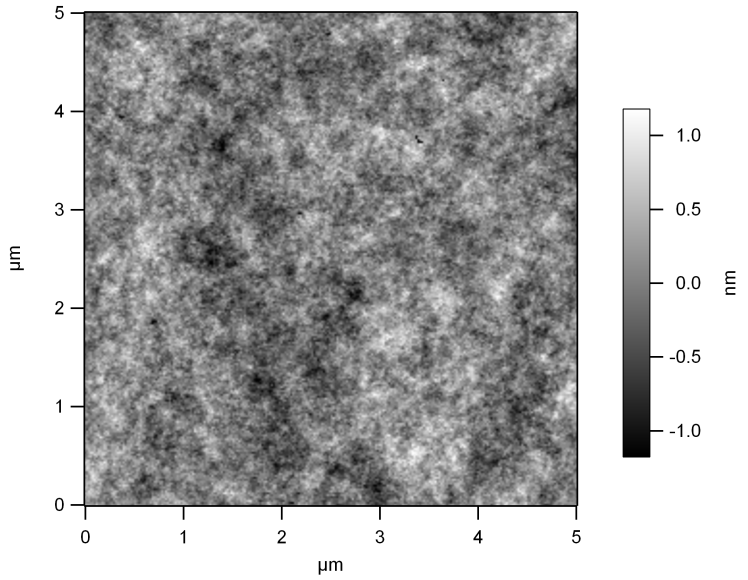

5% P2VP(C_6F_{14})$_2$ and 95% P2VP (annealed)

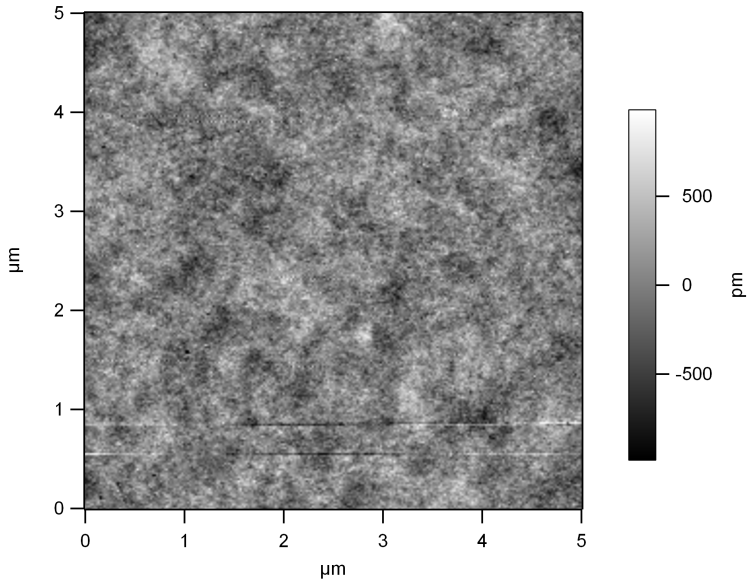

Figure 3.7: AFM images of a mixture 5% P2VP(C_6F_{14})$_2$ and 95% P2VP annealed/not annealed and 5% P2VP(C_6F_{14}) and 95% P2VP annealed/not annealed.

We obtained the same results of the previous images. Pretty flat surfaces, those annealed show a rougher surface than those not annealed. This might be caused by the solvent evaporation in the annealing process.
In some images you can also notice some black spots. Those are due by device artifacts.

2ND System studied

Poly(ethylene oxide) (PEO) can successfully perform as a protein-repellant material, and several studies have demonstrated successful antifouling character when PEO is incorporated into the system.
There are, however, difficulties associated with using PEO as a surface coating. From a processing standpoint, PEO is soluble in water and methods must be administered to anchor it to the protected surface. Furthermore, the high surface energy of PEO prevents it from populating the surface when deposited as a component of a blend or a block polymer. Additionally, PEO offers no synthetic handle for incorporation of backbone functionality.

To address these challenges, a novel strategy can be adobted to decrease the surface energy and add functionality to surface coatings by crosslinking hydrophilic PEO materials with fluoropolymers. By varying the ratio of PEO to fluoropolymer the surface composition can be tuned and correlated with antifouling ability.
By engineering a polystyrene-block-poly[(ethylene oxide)-stat-(allyl glycidyl ether)] (PS-b-P(EO-stat-AGE)) statistical diblock terpolymer where the molar incorporation of AGE is varied.
The pendant alkene of the AGE units can be subsequently functionalized with the chemical moiety of choice. Here we demonstrate the surface characteristics of the polymer after functionalizing AGE repeat units with 1H,1H,2H,2H-perfluoro-octanethiol via thiolene chemistry.

The scheme above (figure 3.8) illustrates the strategy utilized to incorporate functional groups into PEO. Using oxyanionic ring opening polymerization, allyl glycidyl ether (AGE) was copolymerized with EO from an alcohol-terminated polystyrene macroinitiator, PS-OH (1) to yield a statistical diblock terpolymer, PS-b-P(EO-stat-AGE) (2).

Thiolene coupling between 2 and 1H,1H,2H,2H-perfluorooctanethiol was then performed to yield a fluorocarbon-functionalized di-block terpolymer, PS-b-P(EO-stat-fAGE) (3).

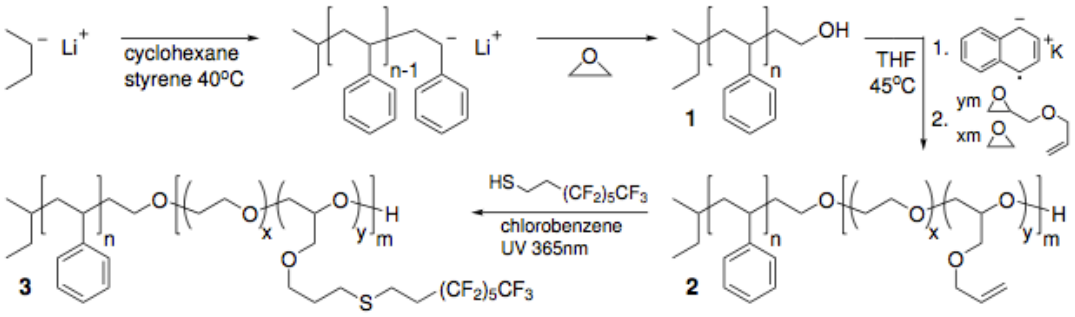

Figure 3.8: Synthesis of PS-b-P(EO-stat-AGE) **2** *via* anionic polymerization followed by modification with *1H,1H,2H,2H perfluorooctanethiol via* thiolene chemistry to give PS-b-P(EO-stat-fAGE) **3.**

An advantage of this strategy is that a series of diblock terpolymers could be synthesized from the same PS-OH macroinitiator with varying polymerization feed ratios of EO to AGE to yield different incorporations of AGE in the P(EO-stat-AGE) block.

So molecules PS-PEO-AGE have been investigated with the AFM instrument. We prepared polymers with different % of AGE: 1%, 3%, 6%, 8% and 16%. And we mix each polymer in Toluene solvent with a concentration 3wt%. After that, we deposited the solution on silica tiles by spin coating technique.

PS-PEO-AGE (1%AGE)

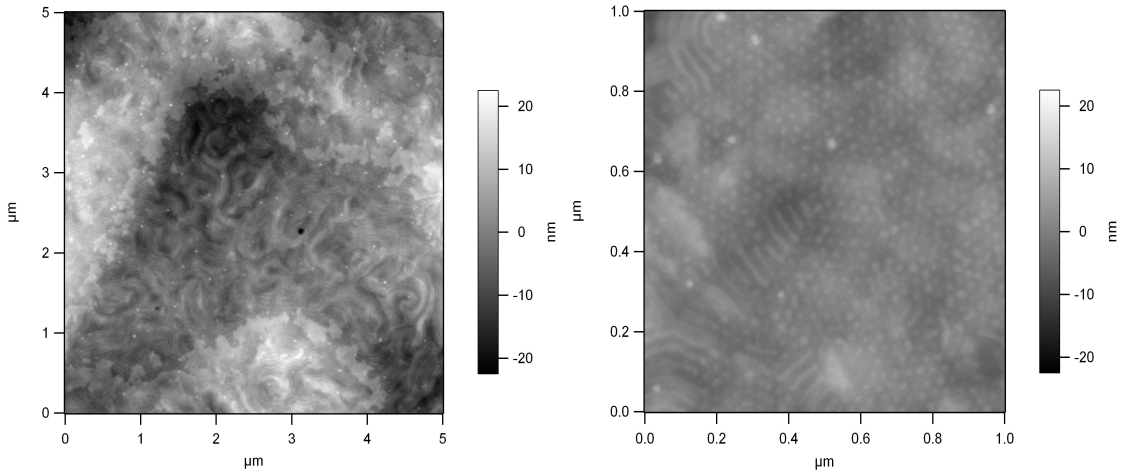

PS-PEO-AGE (3%AGE)

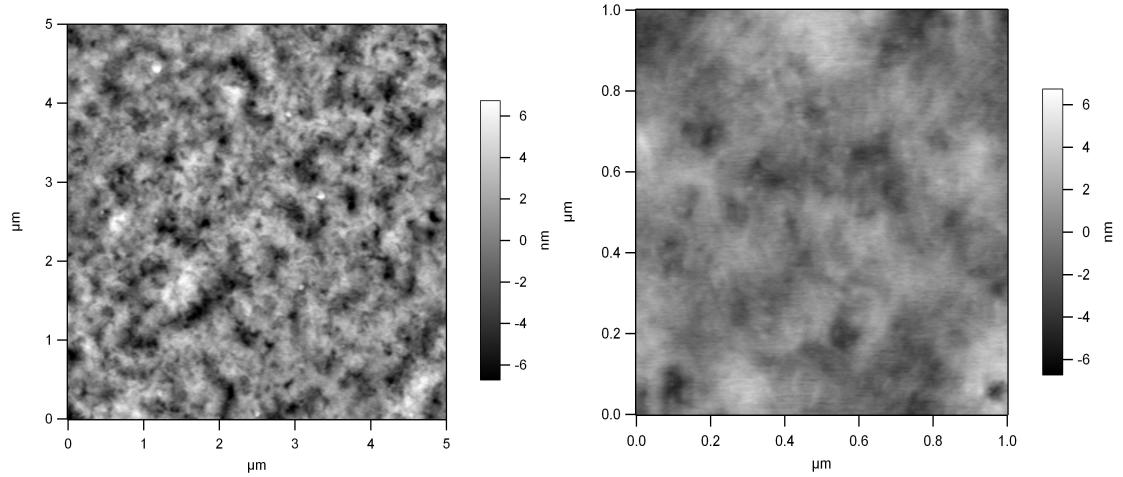

PS-PEO-AGE (6%AGE)

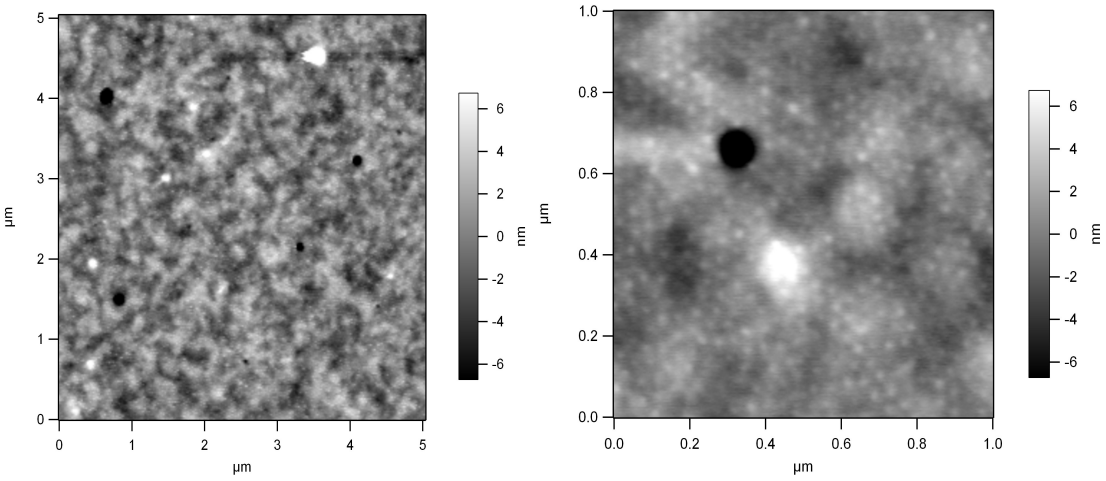

PS-PEO-AGE (8%AGE)

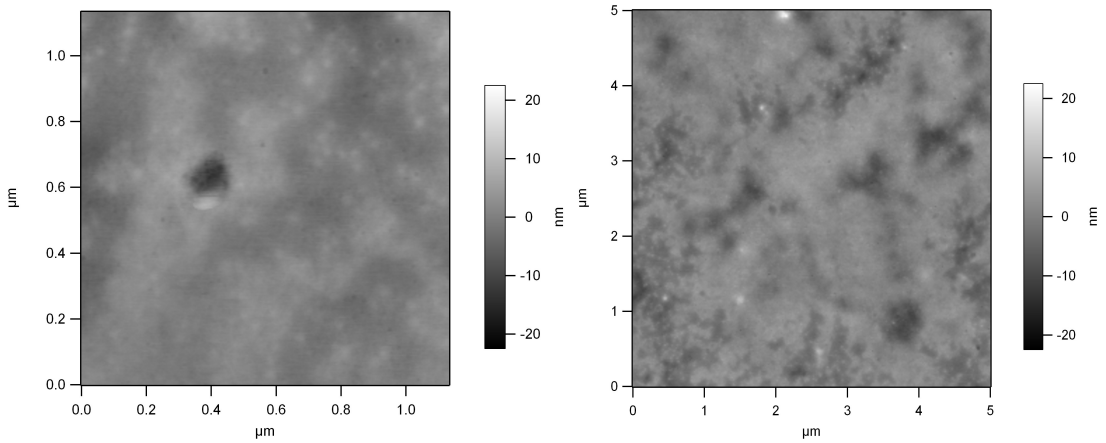

Figure 3.9: AFM images of PS-PEO-AGE molecule with different % of AGE (1%, 3%, 6%, 8%) at different scale.

We have done water contact angle measurements for each sample and we also analyzed the same molecule with age and fluorine arms.

The molecule is PS-b-P(EO-co-fAGE), basically the same molecule (PS-b-P(EO-AGE)) but performed with a fluorocarbon functionalized di-block terpolymer, PS-b-P(EO-stat-fAGE). So in this molecule we also have some fluorine chains attached to the AGE group.

Below, only PS-b-P(EO-co-fAGE) water contact angle measurements are reported, they depict more significant data.

We took measures of advancing and receding angle.

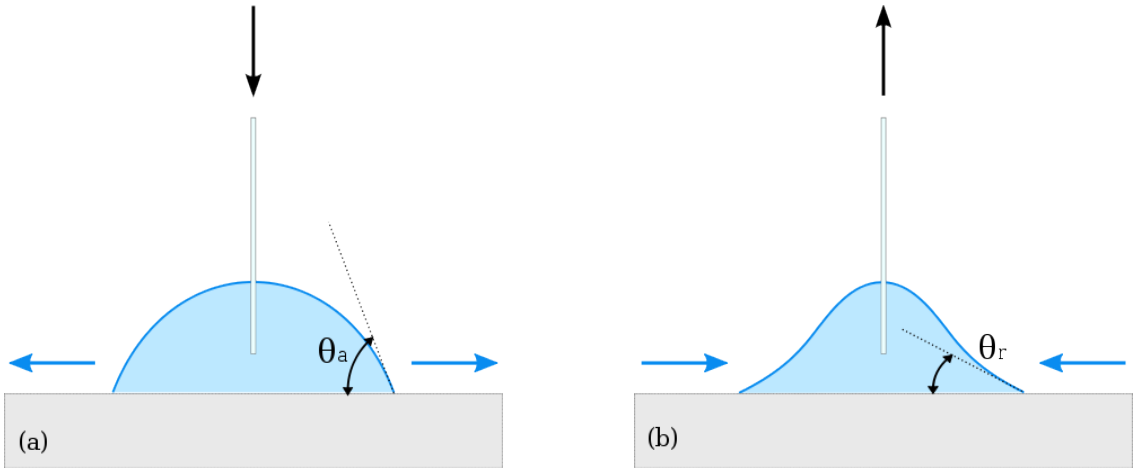

Figure 3.10: Dynamic water contact angle drop method.

For the advancing measurements, we applied a single drop of distilled water to the sample's surface. With a proper syringe we enhanced the amount of water in the drop, so the size of the water drop slightly increased causing the drop to advance. The advancing angle is that angle measured during the drop advance. The measure is not simple; the operator needs to be fast in taking the value of the angle while the edge of the drop is moving. Errors may affect the measure. If a drop is allowed to rest on the surface, the contact angle normally will change a little bit with time, but if such changes are noted, additional measurements should be made.

Regarding the receding angle, with the proper syringe a little amount of water were slightly sucked, in this way the drop tends to recede and the angle can be measured during the drop motion. The measure of this angle is pretty difficult due to the quickly motion of the drop.

By using this technique to measure water contact angles it is possible to develop a picture of the surface reorganization in water, by comparing the advancing and receding contact angles.
This experiment can also serve to monitor reorganization over longer time scales by following the measurements, as the samples remain immersed in water over a period of seven days.

The water contact angle as measured by the water drop technique for the control (AGE0) as well as the two extremes of fluorinated materials (1 mol% - fAGE1 and 16 mol% - fAGE16) are shown in figure 3.11 fAGE samples show a decrease in both receding and advancing contact angles upon the first four hours of submersion in water. This is predominantly due to equilibration of the film when in contact with water and swelling of PEO.

Although initially rapid, this decrease decays, and by two days all films show full equilibration to the aquatic environment. AGE0 however, shows less reorganization and low advancing and receding contact angles that are not consistent with a polystyrene surface. This is likely due to the fact that PEO rapidly swells upon submersion in water and since is the major component of the film, it is able to penetrate the thin PS wetting layer.

It is possible that this reorganization happens at a slower rate for the fAGE films as the hydrophobic perfluoro side chains in the EO-stat-fAGE block slow down the swelling. This is why, ultimately upon equilibration, the advancing contact angle for fAGE1 is higher than AGE0. Similarly, fAGE16 shows considerably higher advancing contact angles than that of fAGE1, which is expected as there is more hydrophobic perfluorinated content on the surface of fAGE16.

The large difference between receding and advancing contact angles for all fAGE films is partially due to the fact that the surfaces are rough, and undergo possible reorganization at the surface when exposed to air or water. This behavior is expected as mixed surfaces comprised of hydrophilic and hydrophobic moieties

have been shown to reconstruct in different environments. The water contact angles show that the surface hydrophobicity, although dynamic in water, can be tuned upon changing the fAGE incorporation.

For each data, we took at least 4/5 measures and we consider the mean value.

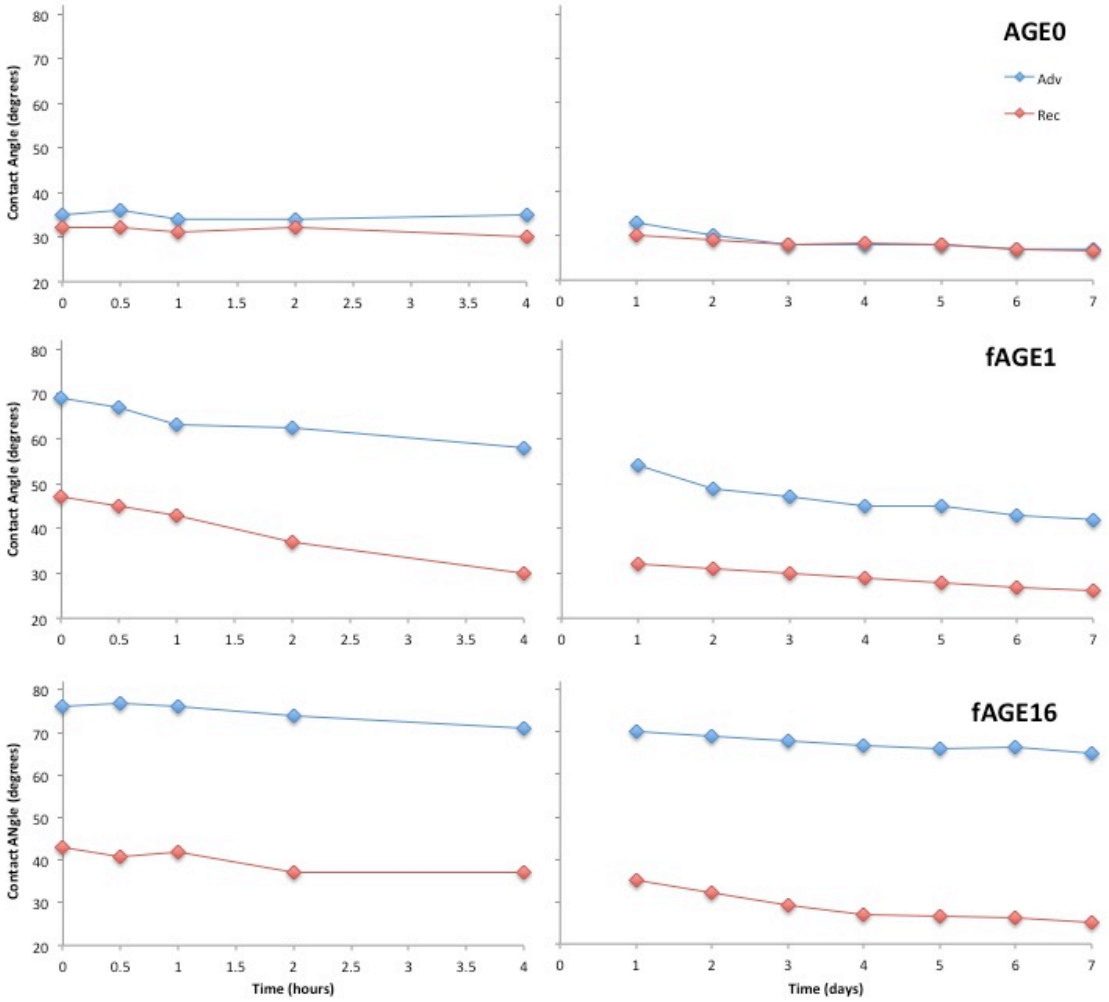

Figure 3.11: Water Contact Angle, advancing and receeding measurements for PS-PEO-fAGE molecule with different % of fAGE.

After the water contact angle measurements, we thought that maybe to expose the surface to the water, some changes might occur. For example the EO has more affinity for water, so it could come up on the surface.

To investigate on that, we double-checked the samples (AGE) with the AFM to see if some changes happened on the surface before and after soaking.

These are the results for the 1mol%, 3mol%:

PS-b-P(EO-AGE) 1mol %

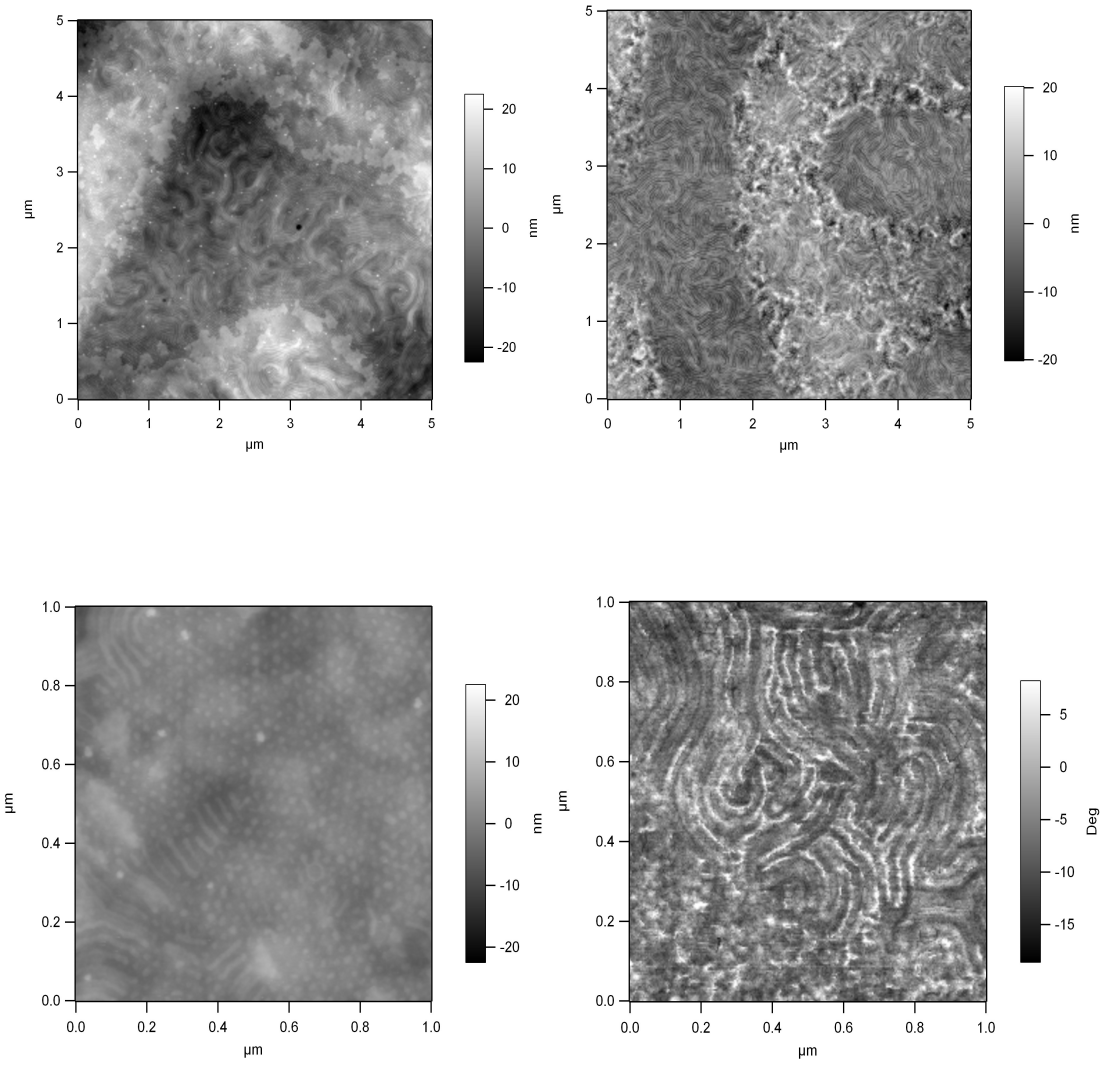

PS-b-P(EO-AGE) 3mol %

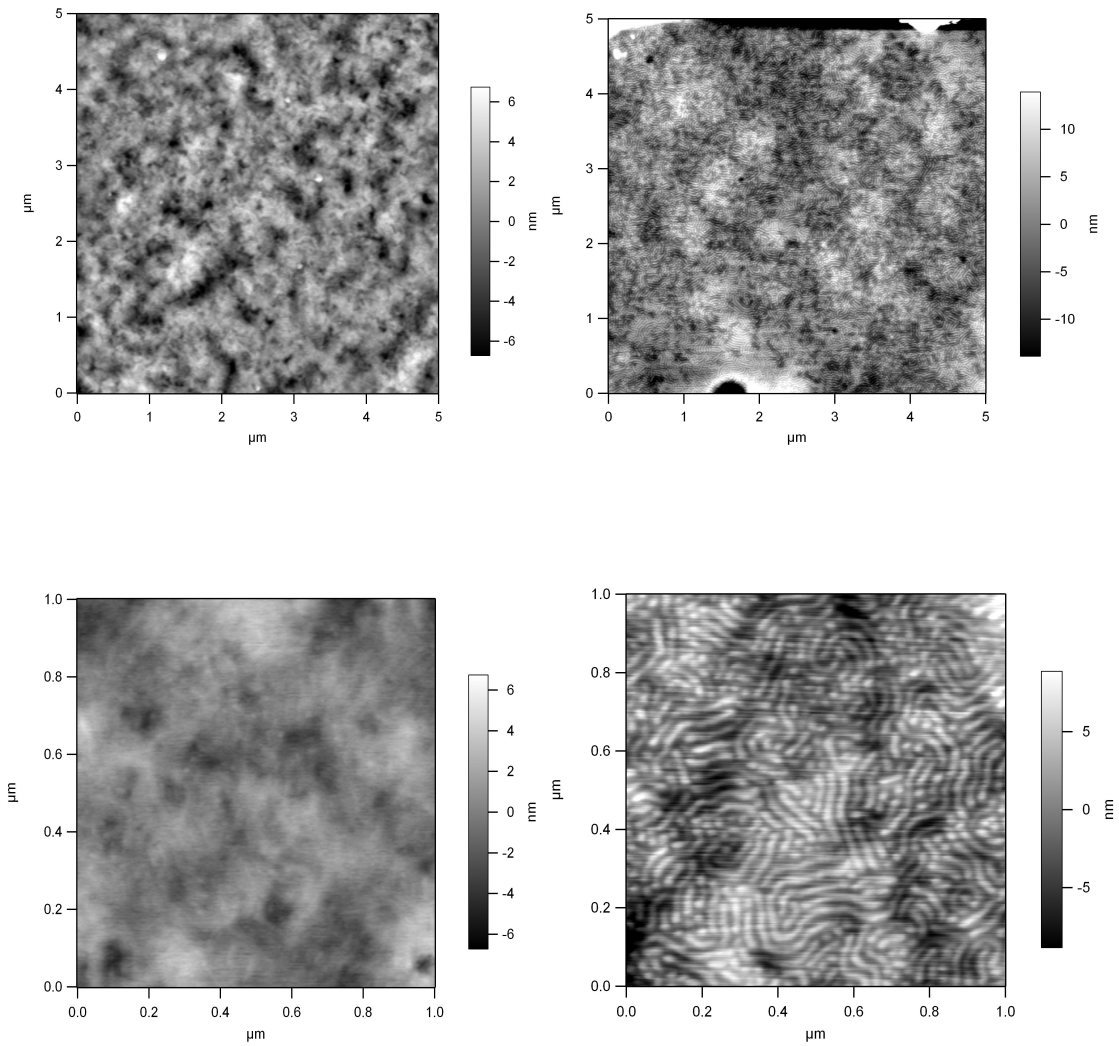

Figure 3.12: AFM images of PS-b-P(EO-AGE) before (a) an after soaking (b) at different scale (5µm and 1 µm).

We repeat the same AFM analysis with PS-b-P(EO-co-fAGE). The pictures below are the AFM images of the sample before and after soaking.

PS-b-P(EO-co-fAGE) 1mol %

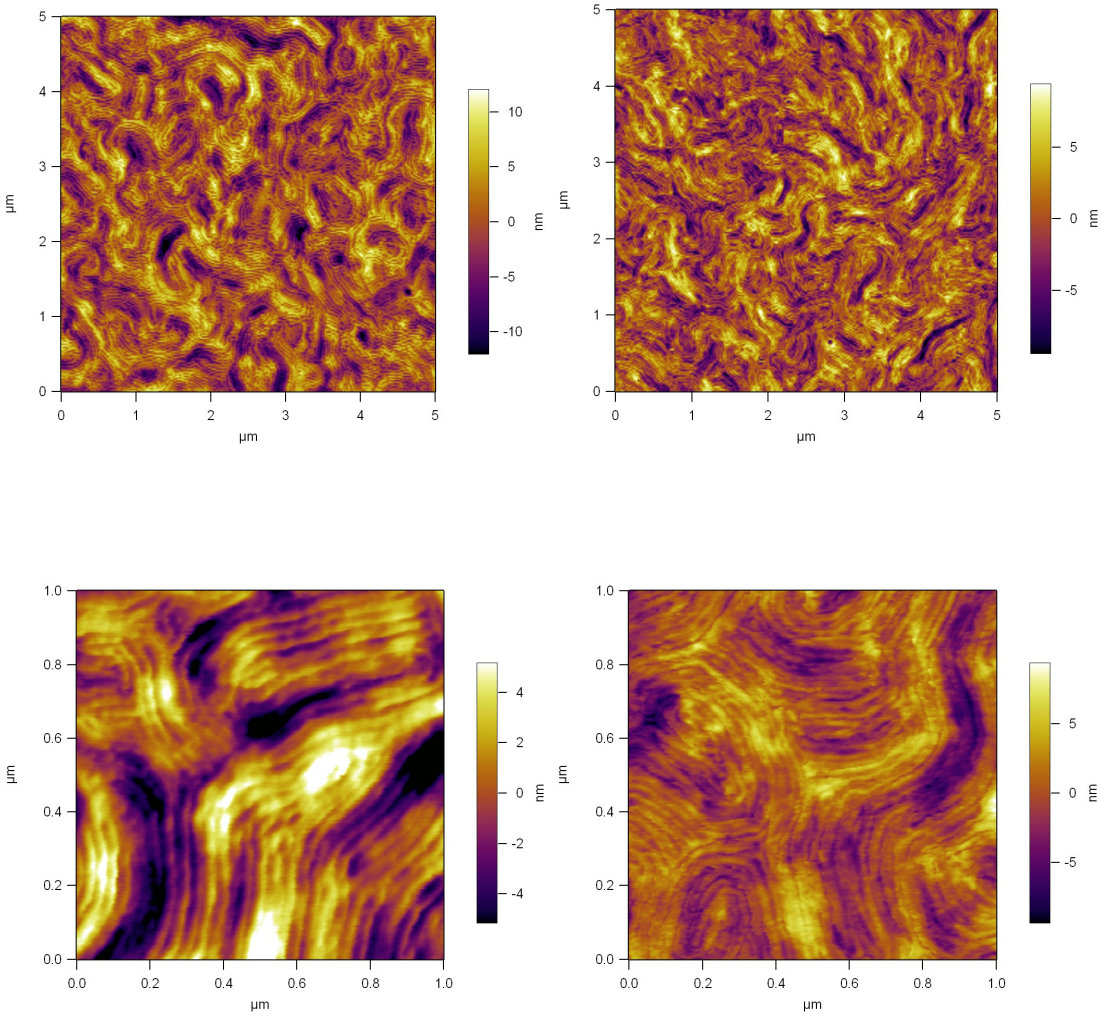

PS-b-P(EO-co-fAGE) 3mol %

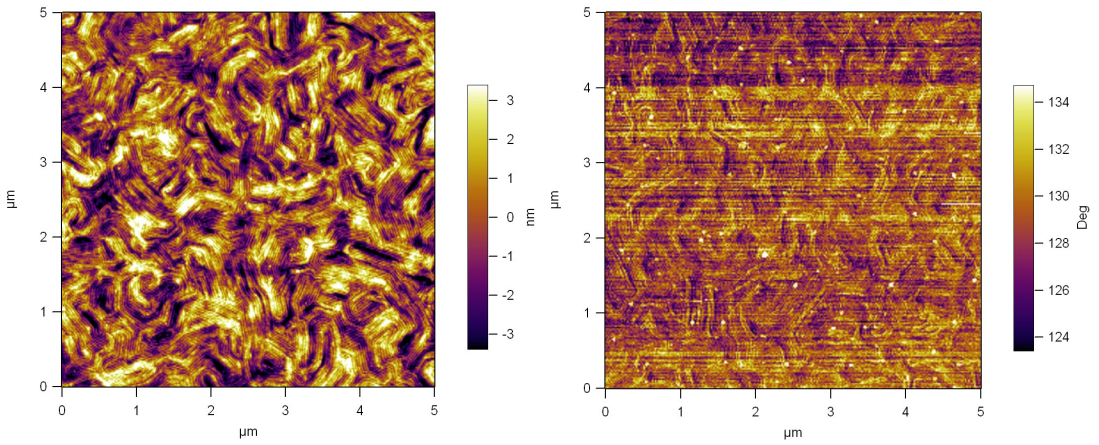

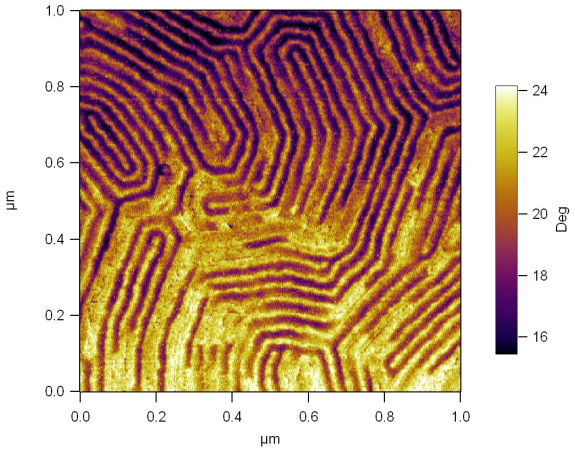

PS-b-P(EO-co-fAGE) 8mol %

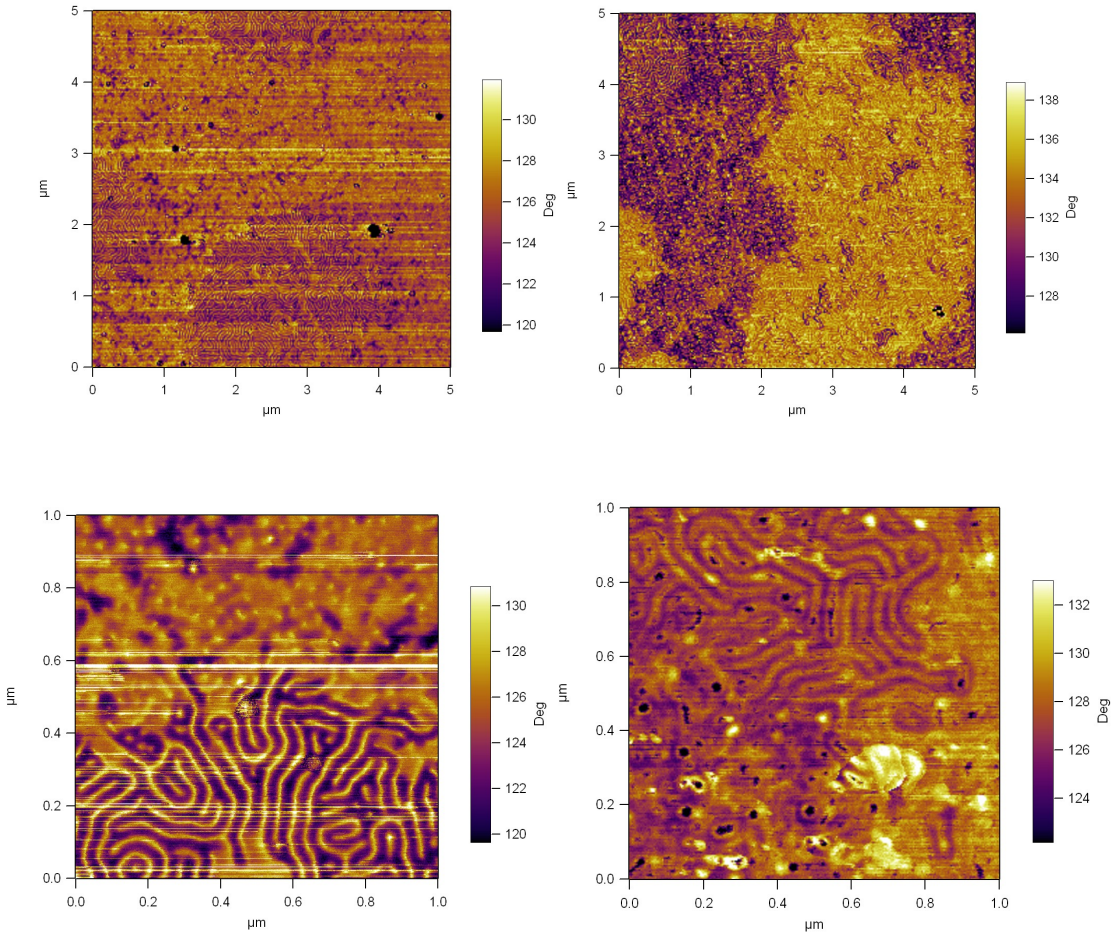

Figure 3.13: AFM images of PS-b-P(EO-AGE) before (a) an after soaking (b) at different scale (5µm and 1 µm).

In all the samples (molecules with only AGE and fAGE) a microphase separation can be noticed. For the AGE only samples, from not soaking to soaking samples there is a partially conversion from perpendicular to parallel domains.
The darker regions represent the lamellar polystyrene domains embedded in a matrix.

In the fAGE images the lamellar domains are even more evident. In the after soaking samples the lamellae tends to assume a parallel configuration. Particulary interesting is the 3 mol% after soaking image, it shows a very straight parallel lamellar domain.

The samples with the fAGE group have been investigated with the XPS.
We took the data at 75° and 0° just to make a comparison between the first 3 nm on the surface and the lower part of the thin film.

XPS measurements were performed using a Kratos Axis Ultra Spectrometer (Kratos Analytical, Manchester, UK) with a monochromatic Al Kα X-ray source (1486.6 eV) operating at 225 W under a vacuum of 1.0 x 10^{-8} Torr.
The data have been manipulated with CasaXPS v.2.3.14 software first and IGOR to plot the graph.

0° and 75° of 0mol % fAGE not soaking (a) and soaking sample (b)

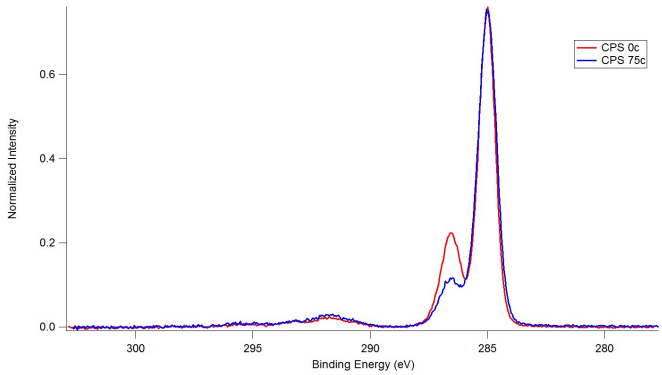

(a)

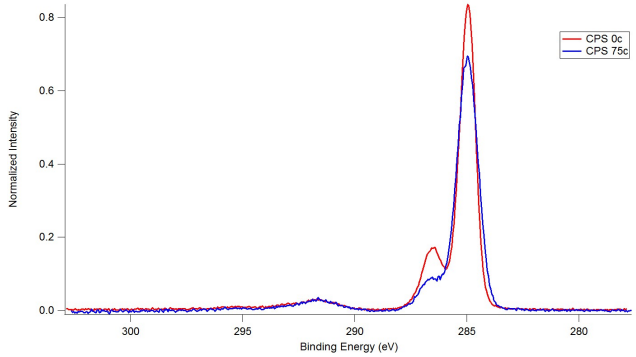

(b)

75° of 0 mol % fAGE not soaking and soaking sample

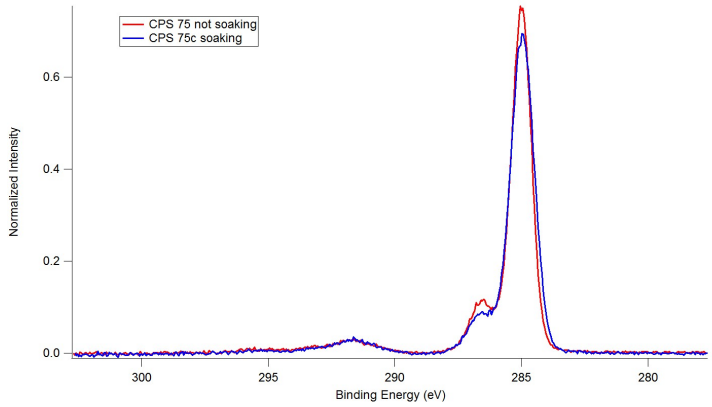

Figure 3.14: XPS of PS-b-P(EO-AGE) (0% fAGE) for soaking (b) and not soaking samples (a).

The spectrum of fAGE 0% displays a strong peak at 285 eV due to electrons from carbons solely bonded to hydrogen and carbon. For the PS-b-PEO system, these chemical bonding states are present in PS, indicating that the surface is predominantly composed of PS.

The broad peak at around 291.5 eV is a π-π* shake-up peak, from the phenyl ring of the PS block, showing that it must be near the surface. The peak at 286.5 eV is due to carbons singly bonded to one oxygen and is representative of the ether carbons of EO units in the system.

Obviously with the 0mol %fAGE there is not the C-F bond in the graph. On the surface (within 3 nm from the top) we have less C-C and C-O bonds.

0° and 75° of 1mol %fAGE not soaking (a) and soaking sample (b)

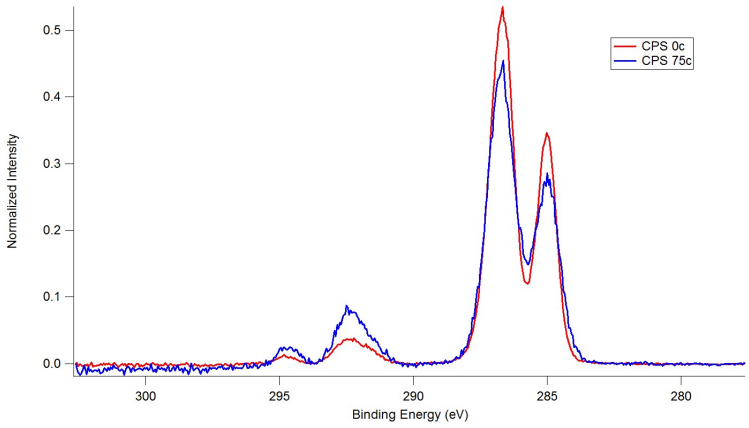

(a)

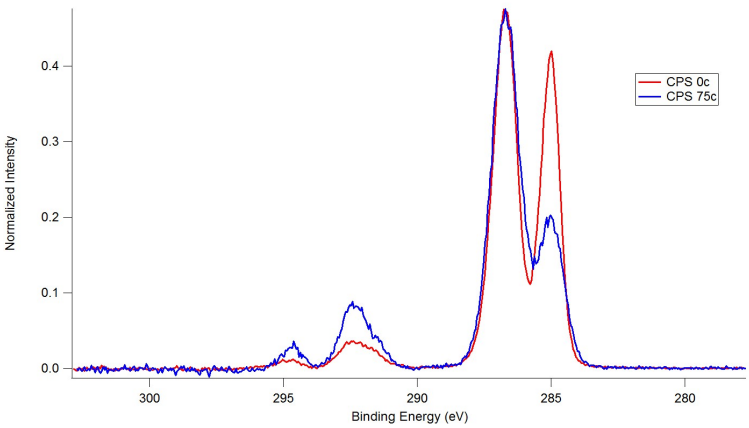

(b)

75° of 1mol % fAGE not soaking and soaking sample

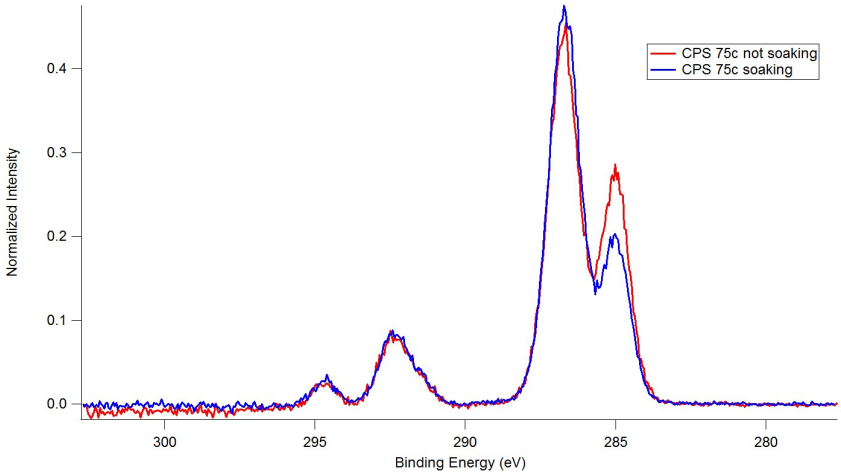

Figure 3.15: XPS of PS-b-P(EO-fAGE) with 1% fAGE for soaking (b) and after soaking (a) samples.

The spectrum of AGE1 is similar to that of AGE0 indicating that the existence of 1mol% AGE in the EO-stat-AGE block does not affect the surface composition when compared to AGE0.

However, by attaching 1H,1H,2H,2H-perfluorooctanethiol to AGE1, yielding fAGE1, the small amount of perfluorocarbon side chains in the system is enough to induce significant changes in the surface composition.

The C1s spectrum for fAGE1 shows a dramatic decrease in the intensity of the peak at 285 eV and a concomitant increase in the ether peak at 286.5 eV. Two new peaks at 292 and 294 eV also appear corresponding to carbons bonded to two fluorine and three fluorine atoms, respectively.

0° and 75° of 3mol %fAGE not soaking and soaking sample

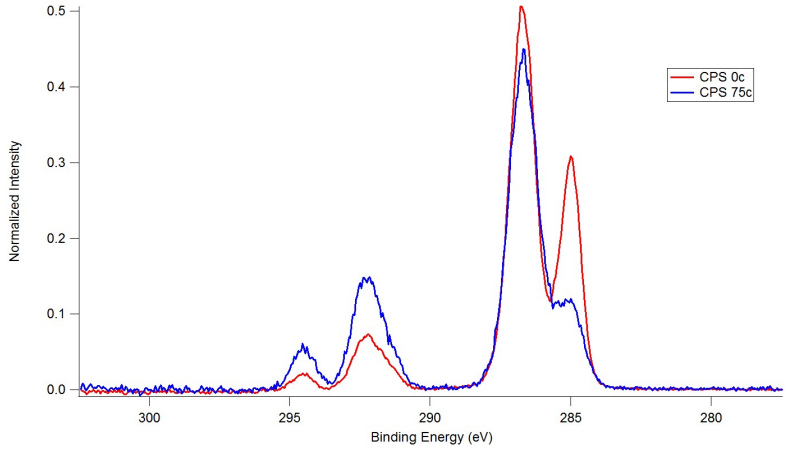

75° of 3mol % fAGE not soaking and soaking sample

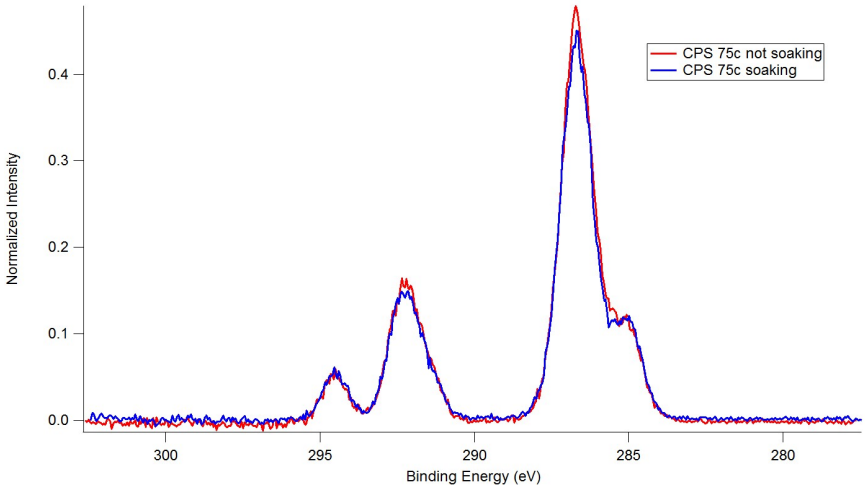

0° and 75° of 6mol % fAGE not soaking (a) and soaking sample (b)

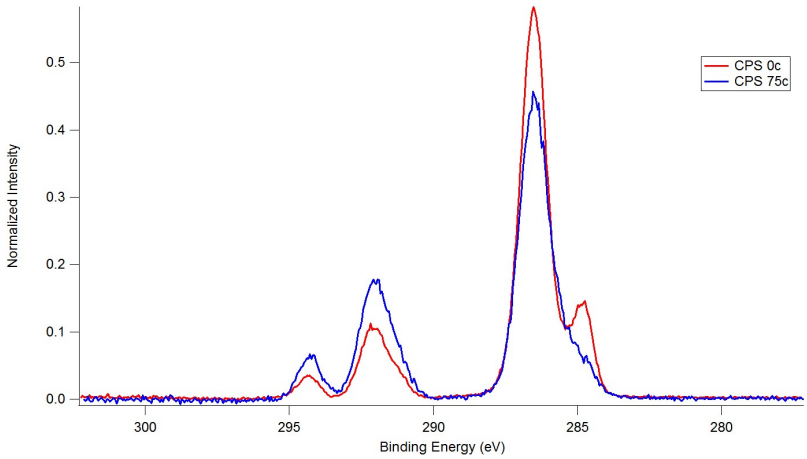

(a)

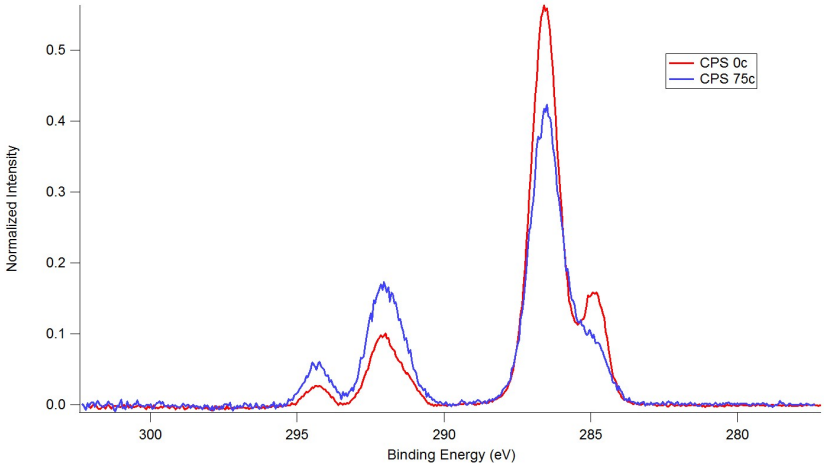

(b)

75° of 6mol % fAGE not soaking and soaking sample

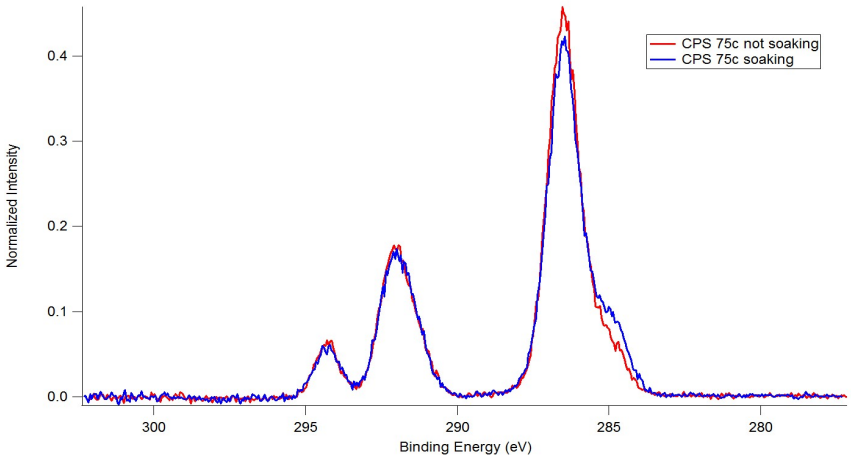

0° and 75° of 8mol % fAGE not soaking (a) and soaking sample (b)

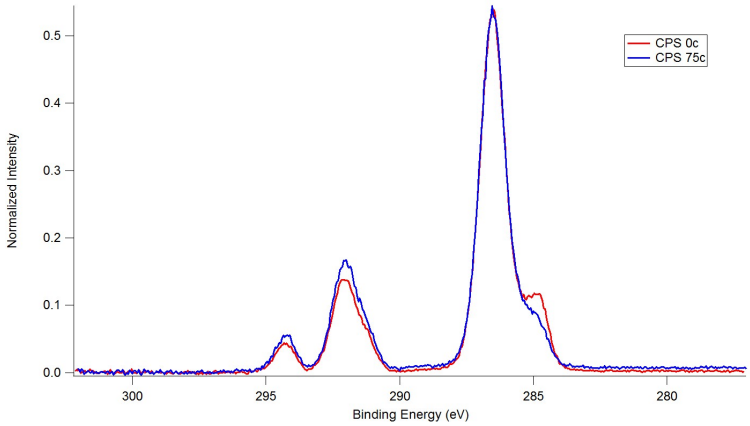

(a)

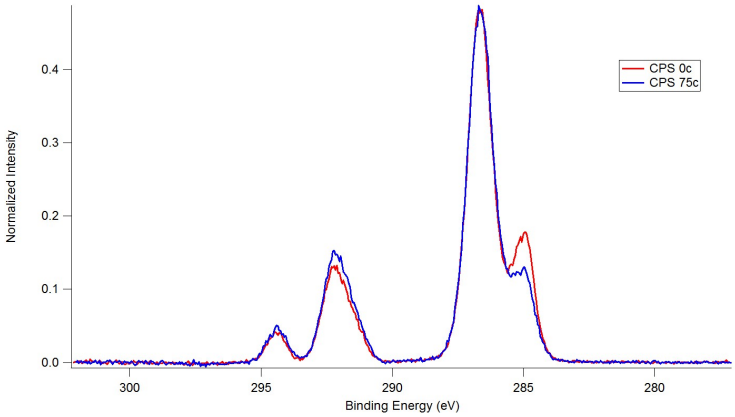

(b)

75° of 8mol % fAGE not soaking and soaking sample

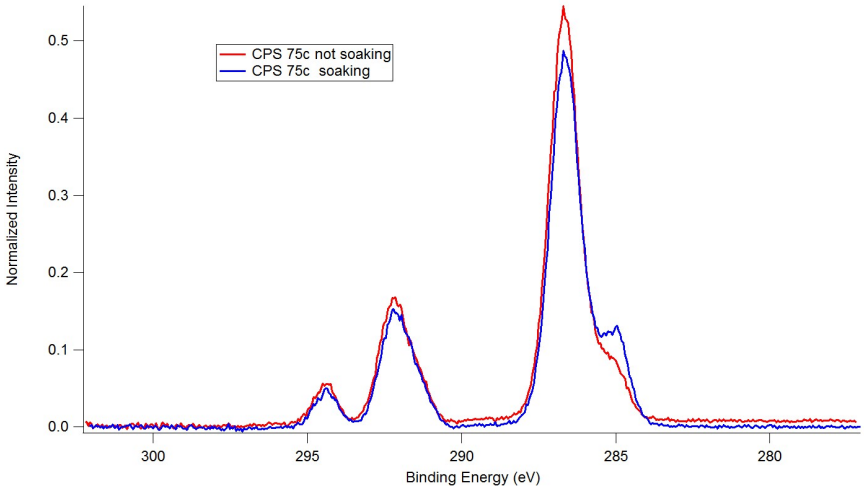

0° and 75° of 16mol % fAGE not soaking (a) and soaking sample (b)

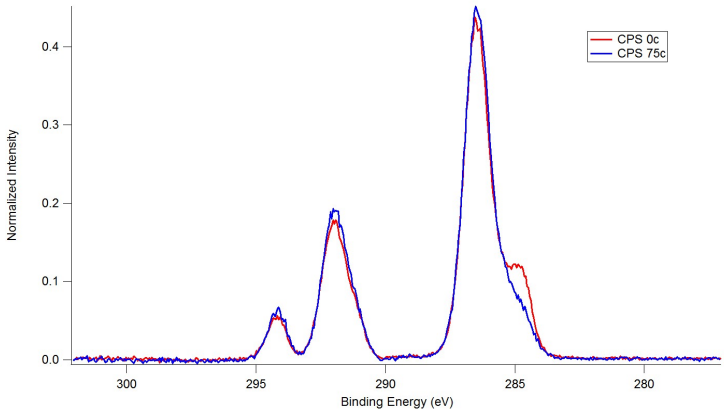

(a)

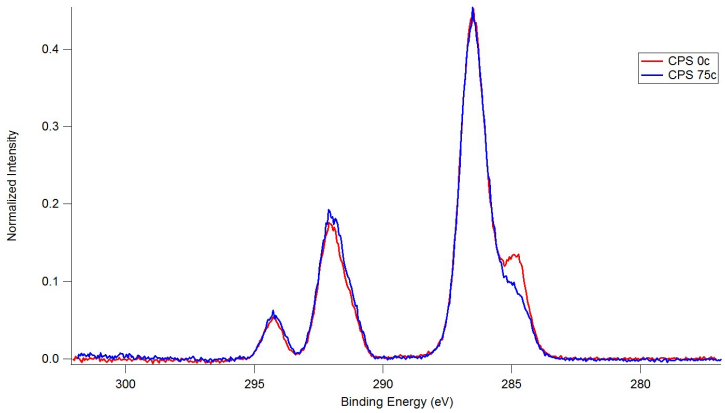

(b)

75° of 16mol % fAGE not soaking and soaking sample

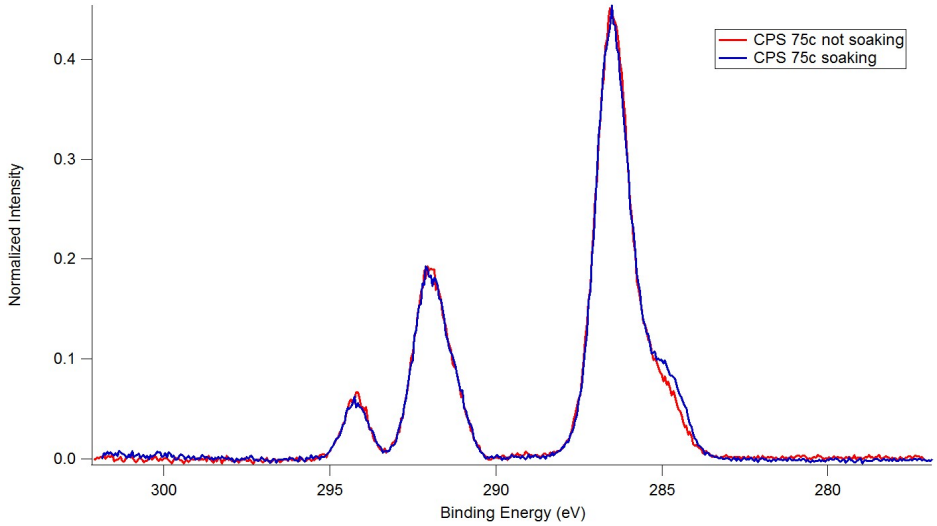

Figure 3.16: PS-b-P(EO-fAGE) at different % of AGE (3%, 6%, 8%, 16%) and before (a) and after soaking (b).

The entire series of fAGE polymers was analyzed by XPS spectroscopy to determine the effect of fAGE incorporation on surface composition.

XPS demonstrates a controlled increase in fluorocarbon content at the surface with increasing incorporation of fAGE (figure 3.17).

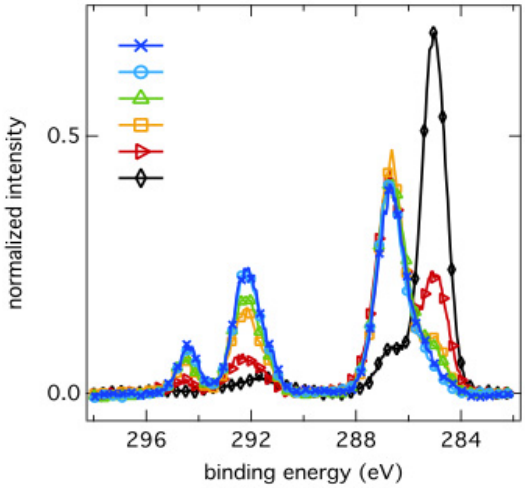

Figure 3.17: Overlay of high resolution XPS spectra of C1s energy range for *fAGE* series recorded at = 75°.

This trend is expected as more perfluorocarbons become available in the EO-stat-fAGE block to populate the surface. The data sets of fAGE8 and fAGE17 show similar spectra indicating that after 8mol% incorporation of fAGE, the surface becomes fully saturated with fAGE. Thus, any additional groups added will not contribute to surface character and exist at depths greater than the penetration depths of XPS.

In conclusion, we though to have more EO on the surface due by EO affinity with water, but we had roughly the same results for both soaking and not soaking samples. The C-C peak of the soaking is a little bit higher than the same peak for the not soaking sample and C-O soaking is a little bit lower. Regarding the fluorinated peaks, they are roughly the same for both soaking and not soaking samples.

Chapter 4

Conclusion

This work focuses on the controlled inclusion of perfluorocarbons into polymer systems using an array of synthetic and processing strategies.
While perfluorocarbon functional groups demonstrate a propensity for segregating to the surface, the underlying theme of this work is to show how these groups alter surface composition and morphology relative to non-fluorinated counterparts.
Such control and application has potential to benefit the coatings, and also lithography and solar cell industries (even though not covered in this work).
With thorough characterization methods, centered around the use of XPS and AFM, the effects of perfluorocarbon addition can be correlated with surface composition and architectural morphologies.

This thesis is part of broader studies in anti-fouling coatings. In these studies, molecules and polymers sinthesys were included.
Controlled synthesis of polymers for antifouling coatings was developed by copolymerizing the functional monomer allyl glycidyl ether (AGE) with ethylene oxide.
With proper modification strategy, polymer was functionalized with fluoro-carbon chains. Analysis by XPS demonstrated precise control over surface concentration by varying the amount of AGE during the polymerization process.

Different receipts (different AGE and fAGE mol %) can lead to different final surface compositions and so different surface properties. Our most important goal was create a material in which we can accurately control the surface composition

by changing the mol % of AGE or fAGE. This has been proven by XPS and AFM analysis.

Next step is to evaluate which surface composition can give better results in anti-fouling. PEO is necessary to prevent protein adsorption which is the first step in many of the foulants attaching to the surface.
Another way that can be adopted is to decrease the surface energy in order to avoid foulants attaching to the surface and so pursuing the fouling release strategy.
This reasult can be achieved using perfluorocarbons on the surface. We can infer a compromise between mol % PEO and mol % fAGE is required to achieve both the properties.

Different samples have to be tested in marine environment against common marine fouling species, in particular green Alga Ulva and diatom Navicula.

Spray coating is a practical method for coating polymers to cover large surface areas and a desirable process for industrial applications.
However, further investigation is warranted to uncover the reorganization mechanism(s) of polymers, especially block copolymers, during the deposition process.
Different receipts have been developed and at the same time it is necessary studying the spray coating method and avoid surface segregation that can lead to modified surface properties.

Bibliography

1. Frederik Wurm, Holger Frey. *"Linear–dendritic block copolymers: The state of the art and exciting perspectives"*. Elsevier. July 2011.

2. I.W. Hamley. *"Ordering in thin films of block copolymers: Fundamentals to potential applications"*. Elsevier June 2009.

3. N. Tirelli, M.P Lutolf, A. Napoli, J.A. Hubbell. *"Poly(ethylene glycol) block copolymers"*. Elsevier 2002.

4. Peter A. George, Bogdan C. Donose, Justin J. *"Cooper-White. Self-assembling polystyrene-block-poly(ethylene oxide) copolymer surface coatings: Resistance to protein and cell adhesion"*. Elsevier 2009.

5. Sergiy Peleshankoa, Vladimir V. Tsukruk. *"The architectures and surface behavior of highly branched molecules".* Elsevier 2008

6. Sitaraman Krishnan, Nick Wang, Christopher K. Ober, John A. Finlay, Maureen E. Callow, James A. Callow, Alexander Hexemer, Karen E. Sohn, Edward J. Kramer, Daniel A. Fischer. *"Comparison of the Fouling Release Properties of Hydrophobic Fluorinated and Hydrophilic PEGylated Block Copolymer Surfaces: Attachment Strength of the Diatom Navicula and the Green Alga Ulva"*. Biomacromolecules. March 2006.

7. Luisa Andruzzi, Emo Chiellini, Giancarlo Galli, Xuefa Li, Seok H. Kang and Christopher K. Ober. *"Engineering low surface energy polymers through molecular design: synthetic routes to fluorinated polystyrene-based block copolymers".* Journal of Materials. April 2002.

8. Dimitriya Bozukova, Christophe Pagnoulle, Marie-Claire De Pauw-Gillet, Nadia Ruth, Robert Jérôme, and Christine Jérôme*. "Imparting Antifouling*

Properties of Poly(2-hydroxyethyl methacrylate)Hydrogels by Grafting Poly(oligoethylene glycol methyl ether acrylate)". Langmuir. February 2008.

9. Luisa Andruzzi, Alexander Hexemer, Xuefa Li, Christopher K. Ober, Edward J. Kramer, Giancarlo Galli, Emo Chiellini, and Daniel A. Fischer. *"Control of Surface Properties Using Fluorinated Polymer Brushes Produced by Surface-Initiated Controlled Radical Polymerization"*. Langmiur. September 2004.

10. Luisa Andruzzi, Wageesha Senaratne, Alexander Hexemer, Erin D. Sheets, B. Ilic, Edward J. Kramer, Barbara Baird, and Christopher K. Ober. *"Oligo(ethylene glycol) Containing Polymer Brushes as Bioselective Surfaces"*. Langmuir. December 2004.

11. Michael Dimitriou. *"Perfluorocarbon Functionality in Polymers: Control of Material Properties and Performance"*. PhD dissertation in materials. September 2011.

12. Craig J. Weinman, John A. Finlay, Daewon Park, Marvin Y. Paik, Sitaraman Krishnan, Harihara S. Sundaram, Michael Dimitriou, Karen E. Sohn, Maureen E. Callow, James A. Callow, Dale L. Handlin, Carl L. Willis, Edward J. Kramer, and Christopher K. Ober. *"ABC Triblock Surface Active Block Copolymer with Grafted Ethoxylated Fluoroalkyl Amphiphilic Side Chains for Marine Antifouling/ Fouling-Release Applications".* Langmuir. June 2009.

13. Daewon Park, Craig J. Weinman, John A. Finlay, Benjamin R. Fletcher, Marvin Y. Paik, Harihara S. Sundaram, Michael D. Dimitriou, Karen E. Sohn, Maureen E. Callow, James A. Callow, Dale L. Handlin, Carl L. Willis, Daniel A. Fischer, Edward J. Kramer, and Christopher K. Ober. *"Amphiphilic Surface Active Triblock Copolymers with Mixed Hydrophobic and Hydrophilic Side Chains for Tuned Marine Fouling-Release Properties".* Langmuir. March 2010

14. Maoliang Xiang, Xuefa Li, Christopher K. Ober, Kookheon Char, Jan Genzer, Easan Sivaniah, Edward J. Kramer, and Daniel A. Fischer. *"Surface Stability*

in Liquid-Crystalline Block Copolymers with Semifluorinated Monodendron Side Groups". Macromelecules. April 2000

15. L.D. Chambers, K.R. Stokes, F.C. Walsh, R.J.K. Wood. *"Modern approaches to marine antifouling coatings"*. Elsevier. August 2009.

16. CAO Shan, WANG JiaDao, CHEN HaoSheng & CHEN DaRong. *"Progress of marine biofouling and antifouling technologies"*. Chinese Science Bulletin. November 2010.

17. Sergiy Peleshankoa, Vladimir V. Tsukruk. *"The architectures and surface behavior of highly branched molecules"*. Elsevier. February 2008.

18. WENJUAN GUO, XINDE TANG, JING XU, XIN WANG, YE CHEN, FAQI YU, MEISHAN PEI. *"Synthesis, Characterization, and Property of Amphiphilic Fluorinated ABC-Type Triblock Copolymers"*. Wiley Online Library. January 2011.